Cell Reports

Article

IL-18-induced HIF-1α in ILC3s ameliorates the inflammation of *C. rodentium*-induced colitis

Graphical abstract

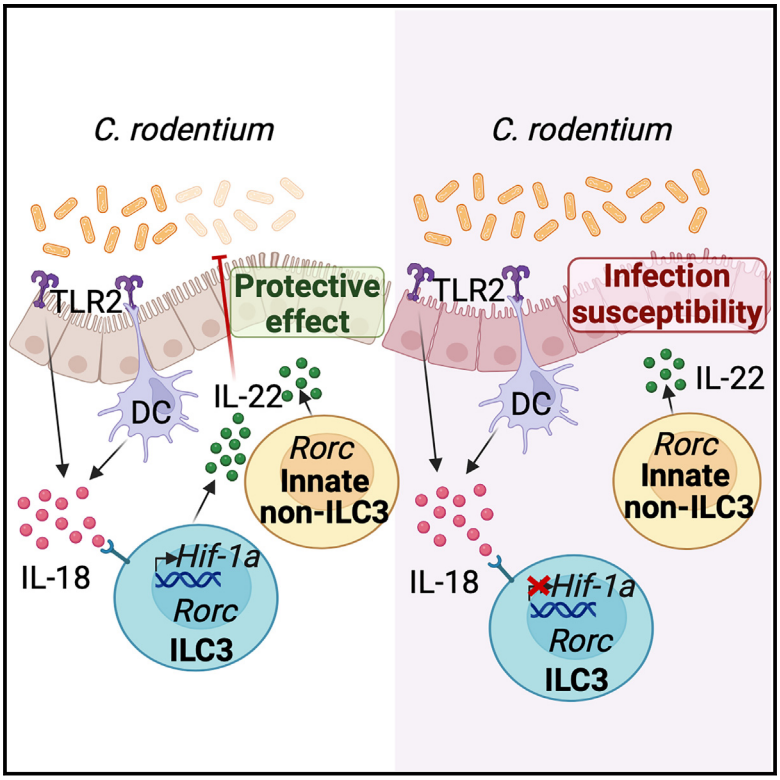

Highlights

- *C. rodentium* induces production of IL-18 in colon, which upregulates HIF-1α in ILC3s
- IL-18 production in the colon is boosted by TLR2 signaling
- HIF-1α promotes IL-22 in ILC3s and not in other innate RORγt$^+$ cells after infection
- IL-18 is responsible for the production of IL-22 by colonic ILC3s through HIF-1α

Authors

Ana Valle-Noguera, Lucía Sancho-Temiño, Raquel Castillo-González, ..., José María González-Granado, Julián Aragonés, Aránzazu Cruz-Adalia

Correspondence

arancruz@ucm.es

In brief

HIF-1α is a hypoxia-inducible factor regulating several immune cells in the response against infections. Valle-Noguera et al. evaluates the function of HIF-1α in colonic ILC3s during *C. rodentium* infection in mice, demonstrating that TLR2-induced IL-18 transcriptionally upregulates HIF-1α in ILC3s, boosting IL-22 secretion to protect against the infection.

Valle-Noguera et al., 2023, Cell Reports *42*, 113508
December 26, 2023
https://doi.org/10.1016/j.celrep.2023.113508

CellPress

Cell Reports

CellPress
OPEN ACCESS

Article

IL-18-induced HIF-1α in ILC3s ameliorates the inflammation of *C. rodentium*-induced colitis

Ana Valle-Noguera,[1,8] Lucía Sancho-Temiño,[1,8] Raquel Castillo-González,[1,8] Cristina Villa-Gómez,[1] María José Gomez-Sánchez,[1] Anne Ochoa-Ramos,[1] Patricia Yagüe-Fernández,[2] Blanca Soler Palacios,[3] Virginia Zorita,[4] Berta Raposo-Ponce,[5] José María González-Granado,[1,7] Julián Aragonés,[6,7] and Aránzazu Cruz-Adalia[1,9,*]

[1]Department of Immunology, Ophthalmology and ENT, School of Medicine, Complutense University of Madrid, Instituto de Investigación Sanitaria Hospital 12 de Octubre (imas12), Madrid, Spain
[2]Centro de Investigaciones Biológicas Margarita Salas (CIB-CSIC), Madrid, Spain
[3]Department of Immunology, Centro Nacional de Biotecnología, Consejo Superior de Investigaciones Científicas (CNB-CSIC), Madrid, Spain
[4]Centro Nacional de Investigaciones Cardiovasculares (CNIC), Madrid, Spain
[5]Centro de Biología Molecular Severo Ochoa (CBM-CSIC), Madrid, Spain
[6]Hospital Santa Cristina, Fundación de Investigación Hospital de la Princesa, Madrid, Spain
[7]CIBER de Enfermedades Cardiovasculares, Instituto de Salud Carlos III, Madrid, Spain
[8]These authors contributed equally
[9]Lead contact
*Correspondence: arancruz@ucm.es
https://doi.org/10.1016/j.celrep.2023.113508

SUMMARY

Group 3 innate lymphoid cells (ILC3s) are vital for defending tissue barriers from invading pathogens. Hypoxia influences the production of intestinal ILC3-derived cytokines by activating HIF. Yet, the mechanisms governing HIF-1α in ILC3s and other innate RORγt$^+$ cells during *in vivo* infections are poorly understood. In our study, transgenic mice with specific *Hif-1a* gene inactivation in innate RORγt$^+$ cells (RAG1KO HIF-1α$^{\triangle Rorc}$) exhibit more severe colitis following *Citrobacter rodentium* infection, primarily due to the inability to upregulate IL-22. We find that HIF-1α$^{\triangle Rorc}$ mice have impaired IL-22 production in ILC3s, while non-ILC3 innate RORγt$^+$ cells, also capable of producing IL-22, remain unaffected. Furthermore, we show that IL-18, induced by Toll-like receptor 2, selectively triggers IL-22 in ILC3s by transcriptionally upregulating HIF-1α, revealing an oxygen-independent regulatory pathway. Our results highlight that, during late-stage *C. rodentium* infection, IL-18 induction in the colon promotes IL-22 through HIF-1α in ILC3s, which is crucial for protection against this pathogen.

INTRODUCTION

Intestinal disorders such as bacterial infections or autoinflammatory diseases negatively affect human health. In affluent nations inflammatory bowel diseases (IBDs) affect over 6 million people, causing significant morbidity in patients. However, in developing countries, enteric bacterial infections, including enteropathogenic *Escherichia coli* (EPEC) and enterohemorrhagic *E. coli* (EHEC), are a common cause of morbidity and mortality, especially in young children.[1,2] The complexity of the molecular mechanisms involved in these affections can be studied *in vivo* with *Citrobacter rondentium* as a mouse model of gastrointestinal infections, IBD dysbiosis, and even tumorigenesis.[3] *C. rodentium* is a gram-negative mucosal pathogen found naturally in mice; it shares some pathogenic pathways with human EPEC and EHEC infections[4] and promotes colonic inflammation and epithelial barrier impairment making it a great model to investigate pathogen-host immune interactions and the pathology of IBDs.[5] The complex physiopathology of gastrointestinal disorders involves several cell populations and numerous signaling pathways within the immune response such as interleukin-22 (IL-22)- and IL-17-expressing CD4$^+$ T cells (Th22 and Th17). Group 3 innate lymphoid cells (ILC3s) constitute one essential innate immune population involved in the response to enteropathogenic infections and IBD development. This subset belongs to the innate lymphoid cells (ILCs), recently discovered cells that lack rearranged antigen-specific receptors.[6–8] Although ILC3s are not the largest population of ILCs in the colon at steady state, they play significant roles in homeostasis and the defense against extracellular pathogens. ILC3s can be subdivided into two subsets defined according to their cell surface expression of natural cytotoxicity receptors, known as NKp46 in mice[7–10]: NKp46$^-$ lymphoid tissue inducer (LTi) cell-like ILC3s and NKp46$^+$ ILC3s that differ in localization and function. NKp46$^-$ LTi-like ILC3s secrete IL-22 and IL-17, whereas NKp46$^+$ ILC3s primarily produce IL-22, which is involved in the containment of intestinal commensals and the innate response to extracellular bacteria such as *C. rondentium*.[11–17] ILC3's main role in the gut includes maintaining the intestinal barrier integrity and promoting mucosal healing,[18] a major clinical endpoint in gastrointestinal disorders

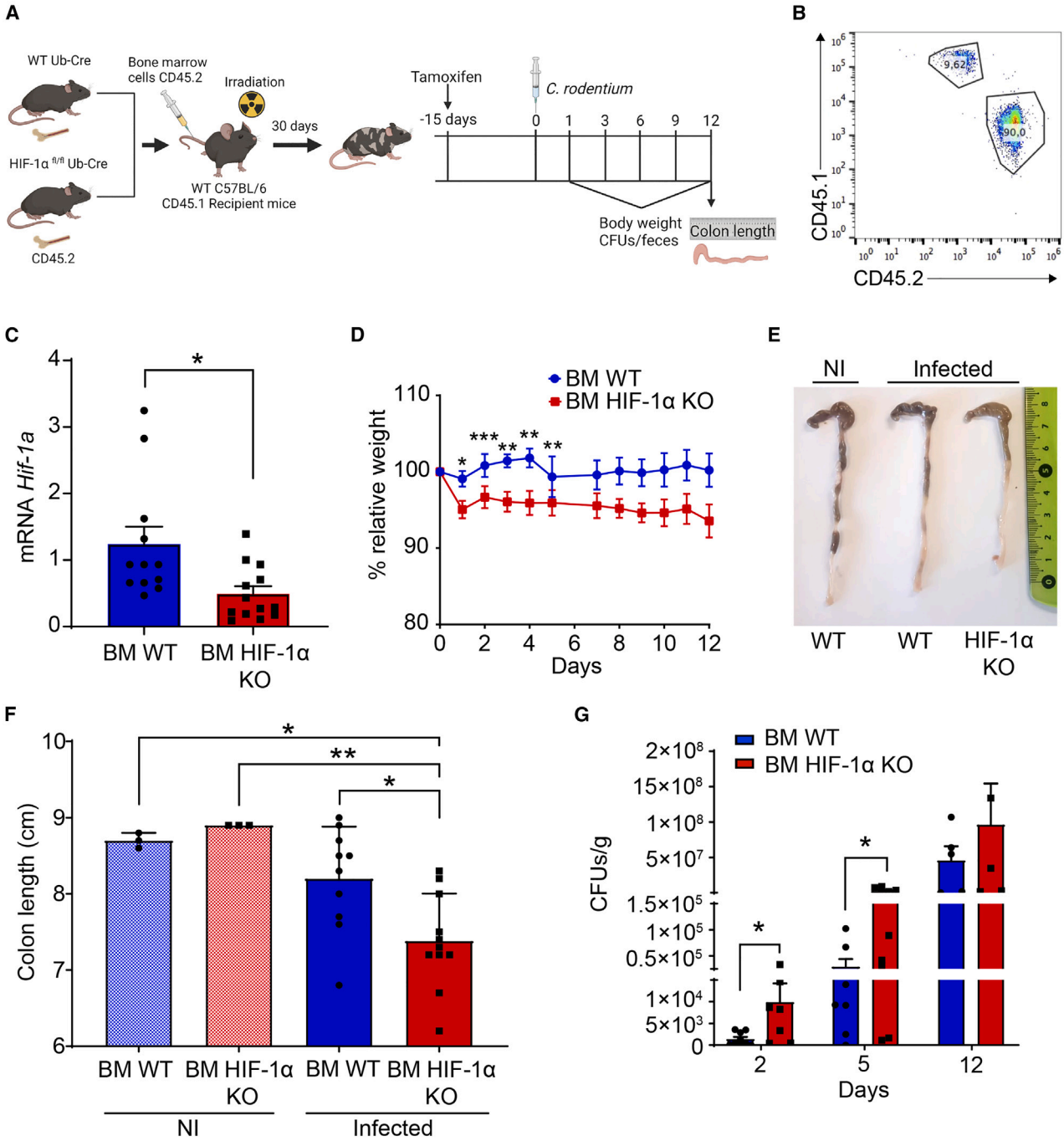

Figure 1. HIF-1α in immune cells is essential for protection against *C. rodentium* infection

(A) Schematic image of the generation of BM chimeras Ub-Cre ERT2 (WT) or HIF-1α$^{fl/fl}$ Ub-Cre (HIF-1α KO) and the experimental procedure of the *C. rodentium* model.

(B) Representative dot plot showing the populations of CD45.1$^+$ and CD45.2$^+$ cells in the peripheral blood of the BM chimeras 4 weeks after BM transplantation.

(C) *Hif-1a* gene expression in the peripheral blood cells of WT and HIF-1α KO BM chimeras.

(D) Relative weight of chimeras WT and HIF-1α KO after *C. rodentium* infection. Representative data of three independent experiments with n = 8.

(E) Image of representative colons of non-infected (NI) and infected chimeras WT and HIF-1α KO after 12 days.

(F) Colon length of the BM chimeras WT and HIF-1α KO 12 days after *C. rodentium* infection.

(G) CFUs of *C. rodentium* in the feces of the chimeras WT and HIF-1α KO 2, 5, and 12 days after infection. Data represent the means ± SD from four (F) or three experiments n = 4 (C and G). Statistical analysis: (C) unpaired t test; (D and G) two-way ANOVA; (F) one-way ANOVA with Sidak multiple comparisons. *p < 0.05, **p < 0.01, ***p < 0.001. Graphs shows individual data.

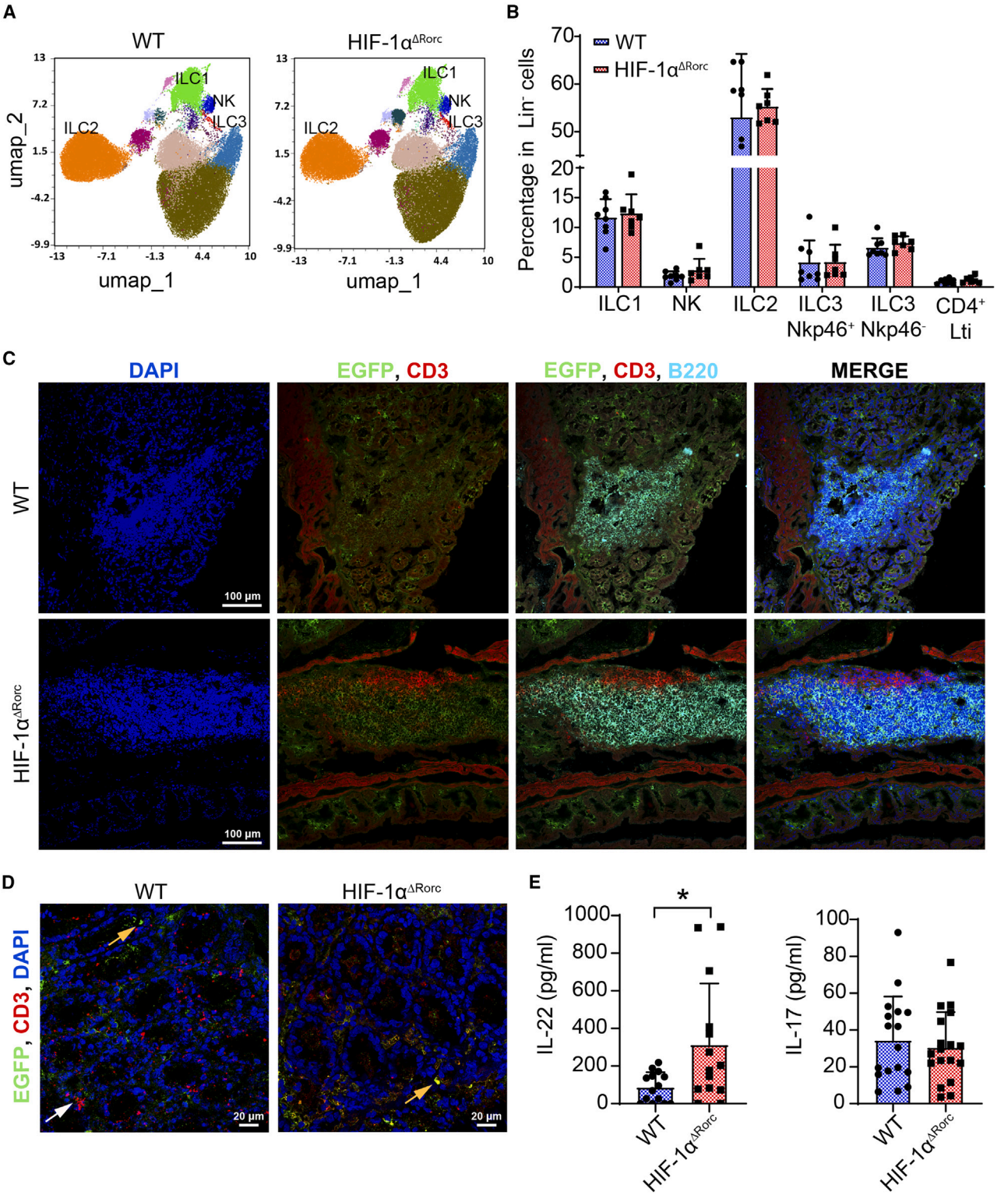

Figure 2. HIF-1α expressed in RORγt⁺ cells does not alter the colonic ILC3 percentage and distribution

(A) Aggregated UMAP visualization of FlowSOM-generated lymphoid cells (linage⁻) of multiparametric flow cytometry data from the colon of the HIF-1α$^{\Delta Rorc}$ and the littermate control (WT). ILC1, ILC2, ILC3, and NK subsets correlate with light green, orange, red, and blue clusters, respectively, according to the expression of several markers (RORγt, EOMES, CD127, KLRG1, and GATA3).

(legend continued on next page)

produced by attaching and effacing pathogens and IBDs.[5,19] ILC3s and Ltis require RORγt for their generation and function. Recent research has identified additional innate non-ILC3 RORγt$^+$ cells in the gut, which are required for the induction of microbiota-specific T regulatory cell differentiation,[20–23] contributing to intestinal homeostasis in steady state.

The molecular mechanisms regulating ILC3s during the development of an infection are currently being investigated. ILC3s can be directly stimulated by cytokines such as IL-23 and IL-1β or TNF-like ligand 1A (TL1A) during colitis.[19,24,25] IL-18 has recently been shown to also play an important role during colitis, secreted by epithelial or innate cells, and necessary for the host defense against *C. rodentium*.[26] In addition, low oxygen levels have been shown to modulate ILC3 response through HIF-1α stabilization.[27] To date, there has been no research into whether HIF-1α in colonic ILC3s is involved in the development of colitis induced by *C. rodentium*, or in relation to what molecular mechanisms, aside from hypoxia, could be modulating this transcription factor during an enteric infection. HIF-1α is not exclusively modulated by oxygen levels; it can also be modulated through pathogen-associated molecular patterns (PAMPs), cytokines, or a combination of factors.[28]

Herein, we study the role of HIF-1α in colonic ILC3s during the physiological condition and during the *C. rodentium* infection model, using specific conditional knockout (KO) mice HIF-1α$^{fl/fl}$RORγtCre (HIF-1α$^{\triangle Rorc}$) and RAG1KO HIF-1α$^{\triangle Rorc}$. The two types of KO mice presented a more severe *C. rodentium*-induced colitis than their control. Interestingly, we found that an innate non-ILC3 RORγt$^+$ population secreted IL-22 in the early phase of the infection but that this secretion was independent of HIF-1α expression (day 5). However, the secretion of IL-22 by colonic ILC3s was regulated via HIF-1α at a later stage of infection (day 12). Moreover, we discovered that, while cytokines IL-1β, IL-23, or TL1A were not responsible for the induction of IL-22 through HIF-1α, IL-18 transcriptionally upregulated HIF-1α in ILC3s, thus promoting a significant induction of IL-22 in WT ILC3s but not in HIF-1α KO cells. Surprisingly, we did not find any difference in the production *in vivo* of IL-17, neither following *C. rodentium* infection in the colon of both types of KO mice nor *in vitro* after the stimulation of HIF-1α KO and WT ILC3s by IL-18 and IL-23. *C. rodentium* can be sensed through the Toll-like receptor 2 (TLR2) by epithelial or innate immune cells, which stimulate the secretion of IL-18, upregulating the expression of HIF-1α in ILC3s and finally activating the production of IL-22. In summary, our findings establish an additional molecular pathway, independent from hypoxia, which can regulate the secretion of IL-22 by colonic ILC3s through HIF-1α, as a target gene of IL-18 signaling, during *C. rodentium* infection.

RESULTS

The expression of HIF-1α in RORγt$^+$ cells is required for defense against *C. rodentium*-induced colitis

HIF-1α is well documented to be expressed in inflamed mucosa, contributing to intestinal homeostasis primarily through its activation in epithelial cells.[29] To investigate the role of HIF-1α within the immune compartment during enteric bacterial infections, we created bone marrow (BM) chimeras, depleting HIF-1α in immune cells using HIF-1α$^{fl/fl}$ Ub-Cre ERT2 mice (referred to as HIF-1α KO), where gene depletion was achieved through tamoxifen exposure (Figures 1A–1C). Remarkably, BM HIF-1α KO chimera mice developed worsened *C. rodentium* colitis, evident in increased weight loss (Figure 1D), greater colon shortening (Figures 1E and 1F), and higher colony-forming units (CFUs) in feces (Figure 1G) compared with control BM Ub-Cre ERT2 (referred to as WT) chimera mice. To explore the specific role of HIF-1α in the innate compartment during colitis, we established mixed BM chimeras by injecting cells from RAG1KO and HIF-1α KO mice (1:1) or RAG1KO and WT control mice (1:1) into recipient mice, thereby re-establishing HIF-1α expression exclusively in the innate compartment (Figures S1A and S1B). Significantly, there were no discernible differences in weight loss (Figure S1C), colon shortening (Figure S1D), or CFUs (Figure S1E) between both sets of chimeras. These findings underscore the critical role of HIF-1α expression in the innate compartment for regulating the development of exacerbated colitis. Given these observations, we sought to investigate the hypothesis that HIF-1α in ILC3 cells plays a pivotal role in the development of *C. rodentium*-induced colitis.

To investigate the role of HIF-1α in ILC3s during *C. rodentium*-induced colitis, we generated mice with HIF-1α gene deletion in RORγt$^+$ cells, crossing HIF-1α$^{fl/fl}$ mice with *Rorc* promoter-driven Cre recombinase mice (*Rorc*-Cre). These conditional KO mice (HIF-1α$^{\triangle Rorc}$) lack the *Hif-1a* gene in RORγt$^+$ cells, including ILC3s, other innate RORγt$^+$ cells, and T cells expressing RORγt during their development in double-positive thymocytes. We also crossed these mice with RORγt EGFP reporter mice to isolate RORγt-expressing cells for further analysis. Quantitative real-time PCR showed that WT HIF-1α$^{fl/fl}$ RORγt EGFP$^{+/-}$ mice (hereinafter WT EGFP$^{+/-}$) expressed more *Hif-1a* mRNA in RORγt$^+$ cells compared with KO HIF-1α$^{\triangle Rorc}$ EGFP$^{+/-}$ mice both in the spleen and the lamina propria of the colon (Figures S2A and S2B). We conducted comprehensive high-dimensional analysis (Figures 2A and S2C) and gating strategies (Figure S2D) to confirm that HIF-1α$^{\triangle Rorc}$ mice did not exhibit differences in the percentage of colonic ILCs under steady-state conditions (Figure 2B). We also considered the presence of other non-ILC3 innate RORγt$^+$ cells,[20–23] which share similarities with myeloid cells, expressing RORγt but not

(B) Flow cytometry analysis of ILC subsets in the colon from the WT and the HIF-1α$^{\triangle Rorc}$.

(C) Representative images of RORγt$^+$ cells (EGFP, green), CD3 (red), and B220 (cyan) immunostaining on colon tissues showing lymphoid follicles from WT EGFP$^{+/-}$ and HIF-1α$^{\triangle Rorc}$ EGFP$^{+/-}$ mice.

(D) Representative images of the lamina propria from the colon of WT EGFP$^{+/-}$ and the HIF-1α$^{\triangle Rorc}$ EGFP$^{+/-}$. Orange arrows show innate RORγt$^+$ cells (EGFP$^+$ CD3$^-$) and the white arrow indicates T cells (CD3$^+$).

(E) IL-22 and IL-17 protein secretion by colon explants cultured *ex vivo* for 24 h. Individuals/means ± SD for each sample from three independent experiments, with n = 5 (B and E). Statistical analysis: (B) two-way ANOVA with Sidak's multiple comparisons; (E) unpaired t test. *p < 0.05. Symbols represent individual animals.

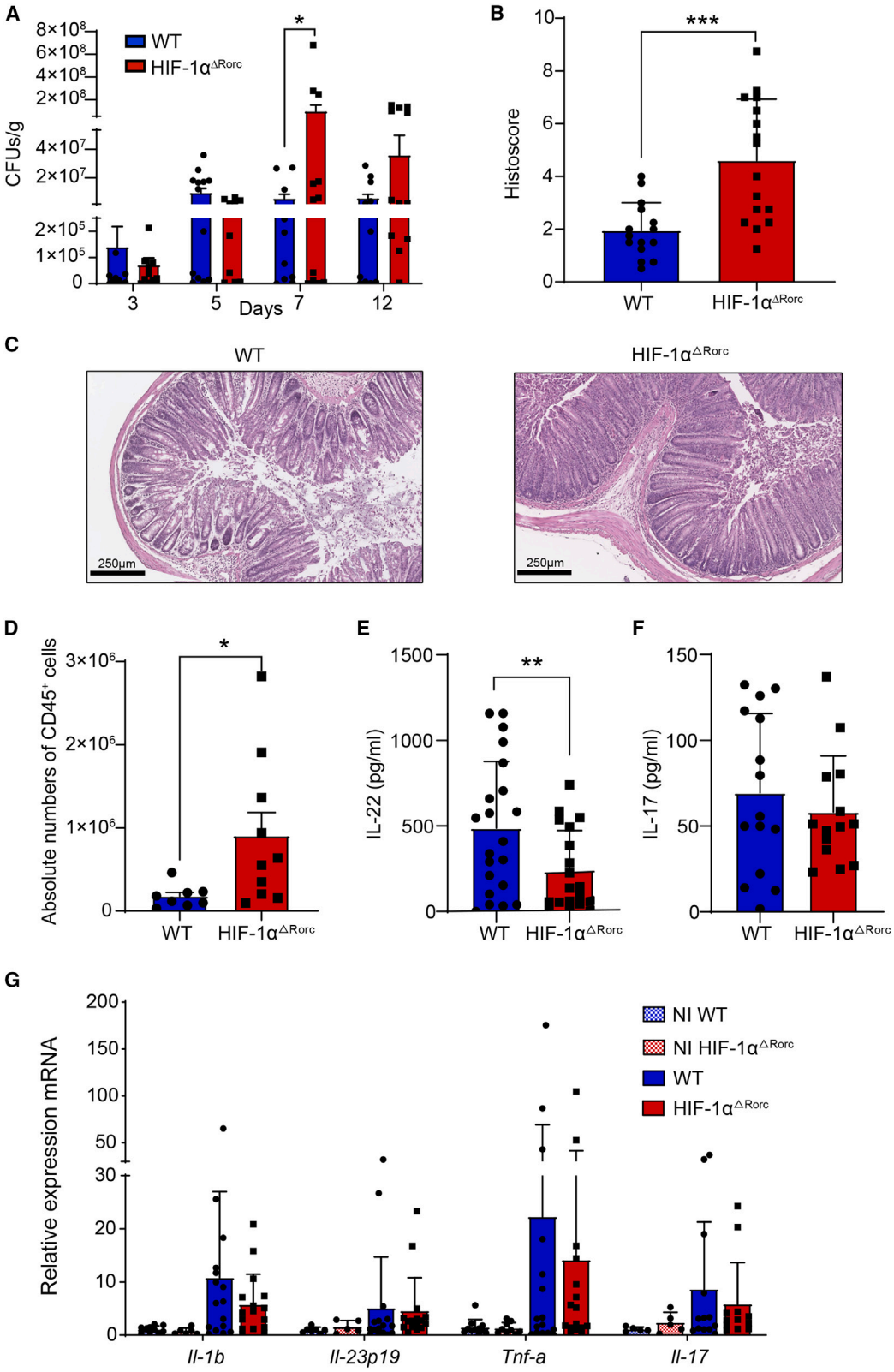

(legend on next page)

CXCR6, IL-7R, or CD90 (Figure S2E). This analysis revealed no differences in the cell number of this population between the two strains (Figure S2F). In addition, the absolute numbers of various RORγt-expressing populations in the spleen were similar in HIF-1α$^{\Delta Rorc}$ and control mice (Figure S2G). Confocal microscopy analysis demonstrated a comparable distribution of colonic CD3$^-$RORγt$^+$ cells in both transgenic mice within lymphoid follicles (Figure 2C) and the lamina propria of the colon (Figure 2D). However, a significant increase in IL-22 protein induction was observed in the colons of HIF-1α$^{\Delta Rorc}$ mice compared with control mice, although no difference was detected in IL-17 levels (Figure 2E). Furthermore, histological analysis of the colon in these conditional mice did not reveal any signs of pathology in the baseline condition (Figures S3A and S3B).

To assess colitis development in these conditional mice following infection, we employed the *C. rodentium* colitis model, which relies on ILC3s during the acute phase.[30] Surprisingly, HIF-1α$^{\Delta Rorc}$ mice displayed more severe colitis compared with their controls. Despite having elevated baseline IL-22 levels in the colon (Figure 2E), these mice exhibited increased CFUs in their feces (Figure 3A) and more pronounced colon inflammation, as assessed by histoscore and flow cytometry (Figures 3B–3D). However, no significant difference was observed in terms of weight loss (Figure S3C). Of significance, a notable reduction in IL-22 protein induction was observed in the colons of HIF-1α$^{\Delta Rorc}$ mice 12 days post-infection in contrast to the control mice (Figure 3E), potentially explaining the increased disease severity in HIF-1α-deficient mice. Conversely, other cytokines such as IL-17 (Figures 3F and 3G) remained unaffected in these conditional mice. There were no significant alterations in the mRNA expression of *Il-1b*, *Il-23p19*, and *Tnf-a* (Figure 3G). Concerning the formation and maintenance of lymphoid structures, the number of colonic patches in both non-infected and *C. rodentium*-infected colons was unaltered in HIF-1α$^{\Delta Rorc}$ compared with control mice (Figure S3D). Furthermore, no differences were observed in the localization of ILC3s within colon lymphoid follicles after 12 days of infection (Figure S3E).

Deficiency of HIF-1α in innate RORγt$^+$ cells impairs IL-22 induction during *C. rodentium* infection, exacerbating colitis

To further evaluate the *in vivo* impact of HIF-1α specifically expressed in innate RORγt$^+$ cells in the *C. rodentium*-colitis model, we crossed the HIF-1α$^{\Delta Rorc}$ mice with the RAG1KO mice to obtain RAG1KO HIF-1α$^{\Delta Rorc}$ mice to eliminate any possible contribution by HIF-1α in T cells. We observed no differences either in the percentage of colonic ILCs (Figure S4A) or in histology analysis in RAG1KO HIF-1α$^{\Delta Rorc}$ mice compared with the littermate control RAG1KO WT mice in steady state (Figures S4B and S4C). Subsequently, we evaluated the impact of deficient expression of HIF-1α in ILC3s in the *C. rodentium*-colitis model, observing that the RAG1KO HIF-1α$^{\Delta Rorc}$ exhibited lower survival rate than their littermate controls (Figure 4A) as well as a significantly greater weight loss (Figure 4B). Interestingly, we observed that the CFUs in the feces of the RAG1KO HIF-1α$^{\Delta Rorc}$ mice showed a declining trend in the first few days of infection, but that effect subsequently became inverted (Figure 4C). Indeed, when we measured IL-22 expression in the colon, a trend of more protein levels was detected in the colon of the RAG1KO HIF-1α$^{\Delta Rorc}$ mice compared with the control under physiological conditions (Figure 4D), which explained the decrease in CFUs observed in the RAG1KO HIF-1α$^{\Delta Rorc}$ mice the first days of infection. However, induction of IL-22 12 days after *C. rodentium* infection became impaired in these deficient mice (Figure 4D), with results similar to those observed in the HIF-1α$^{\Delta Rorc}$ mice (Figure 3E). Moreover, histology score clearly showed that the RAG1KO HIF-1α$^{\Delta Rorc}$ mice developed more severe inflammation in the colon than the control mice (Figures 4E and 4F). In combination, these experiments demonstrate a key role of cell-intrinsic HIF-1α in regulating the production of IL-22 by colonic innate RORγt$^+$ cells, thus preventing a more severe colitis.

HIF-1α regulates the production of IL-22 in ILC3s after *C. rodentium* infection

To ascertain whether the impaired induction of IL-22 in this colitis model was a consequence of the deletion of HIF-1α in the ILC3s or in other RORγt$^+$ cells, we assessed in which cell types IL-22 was affected in the HIF-1α$^{\Delta Rorc}$ mice after 2, 5, and 12 days of infection. On day 2, there was a notable increase in IL-22$^+$ cells in Lin-CD3$^-$RORγt$^+$ NKp46$^-$ IL-7R$^+$ CXCR6$^+$ CD90$^{+/-}$ populations (which include Lti and ILC3 NKp46$^-$) in the colon of HIF-1α$^{\Delta Rorc}$ mice. In addition, the CD3$^-$ RORγt$^+$ IL-7R$^-$ CXCR6$^-$ CD90$^-$ subpopulation (referred to as non-ILC3 innate RORγt$^+$ cells) also showed IL-22 production after 2 days of infection (Figure 5A). No significant differences were observed in the cell counts for ILC3s or the non-ILC3 innate RORγt$^+$ cells between WT and HIF-1α$^{\Delta Rorc}$ mice (Figure 5B). On day 5 of infection, no difference was observed in the percentage of any ILC3 and Lti IL-22$^+$ subpopulations (Figure 5C). Regarding the non-ILC3 innate RORγt$^+$ cells, these produced high levels of IL-22 5 days after infection, but no difference was detected between the HIF-1α$^{\Delta Rorc}$ and WT mice (Figure 5C). As we observed in the IL-17 production by colon explants, the percentage of IL-17-positive cells in the ILC3s was similar in these transgenic mice (Figure S4D). Unlike IL-22 (Figure 5C), the non-ILC3 innate

Figure 3. HIF-1α, expressed in RORγt$^+$ cells, is important for protection against *C. rodentium* infection

(A) CFUs of *C. rodentium* in feces from the HIF-1α$^{\Delta Rorc}$ and the littermate control mice (WT) after infection.

(B) Histoscore of the colitis in HIF-1α$^{\Delta Rorc}$ and WT mice 12 days after *C. rodentium* infection.

(C) Representative image of H&E staining on colon tissues from an infected WT and HIF-1α$^{\Delta Rorc}$ mouse stained with H&E.

(D) Absolute number of CD45$^+$ cells isolated from the lamina propria of the colon from the HIF-1α$^{\Delta Rorc}$ and WT mice 5 days after *C. rodentium* infection.

(E and F) IL-22 and IL-17 protein secretion by colon explants from *C. rodentium*-infected HIF-1α$^{\Delta Rorc}$ and WT mice on day 12.

(G) mRNA relative expression of several cytokine genes in the colon from HIF-1α$^{\Delta Rorc}$ and WT mice non-infected (NI) and 12 days after infection. The data represent the means ± SD from three independent experiments with n = 5/6. Statistical analysis: (A and G) two-way ANOVA, Sidak's multiple comparison test; (B) Mann-Whitney U test; (D–F) unpaired t test. *p < 0.05, **p < 0.01, ***p < 0.001. Symbols represent individual animals.

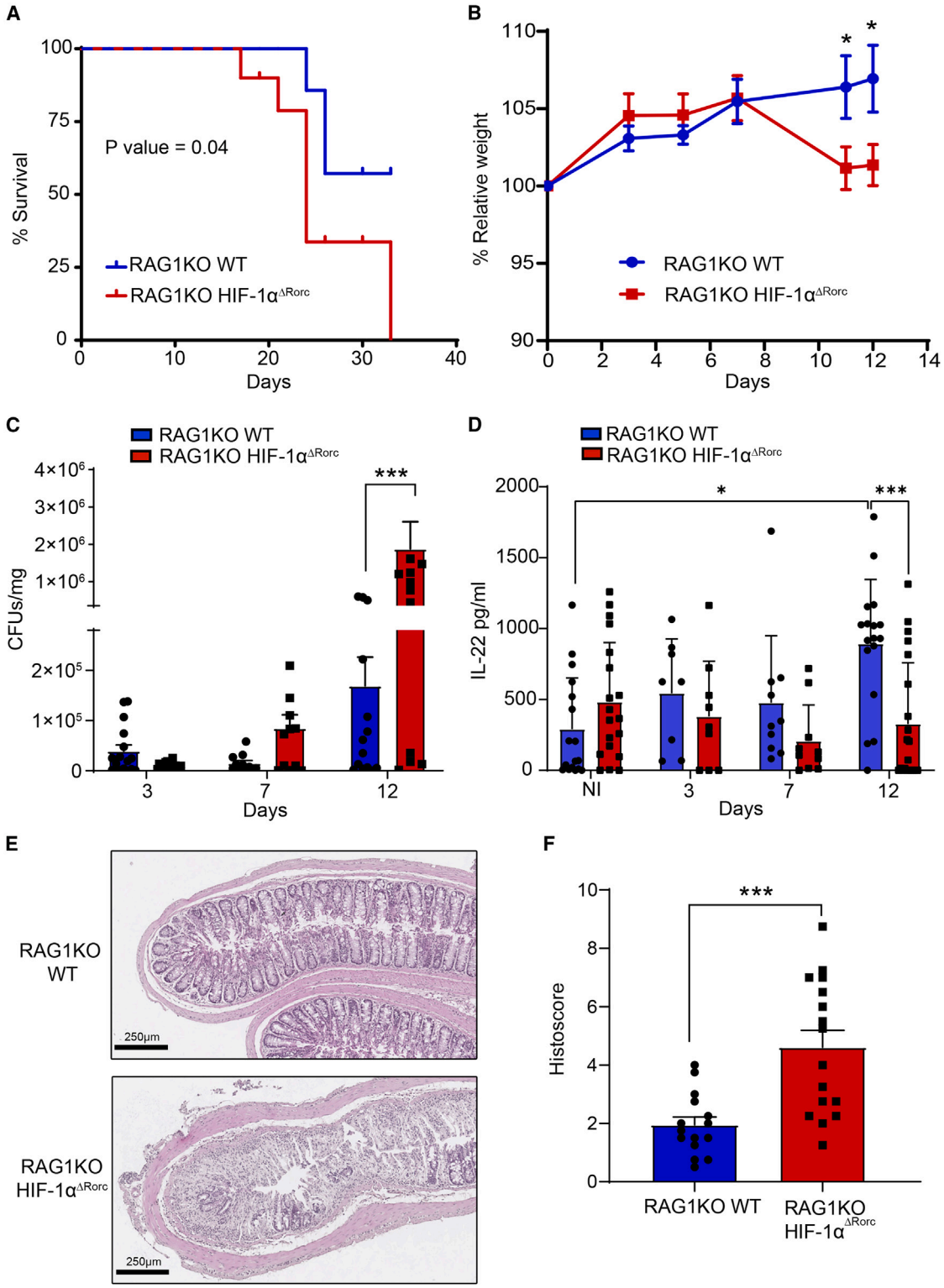

Figure 4. HIF-1α expressed in ILC3 RORγt$^+$ cells protects against severe colitis induced by *C. rodentium*

(A) Survival rate of RAG1KO HIF-1α$^{\Delta Rorc}$ and RAG1KO WT control mice after *C. rodentium* inoculation, n = 7.

(B) Relative weight of RAG1KO HIF-1α$^{\Delta Rorc}$ and RAG1KO WT mice after *C. rodentium* infection.

(C) CFUs of *C. rodentium* in the feces from RAG1KO HIF-1α$^{\Delta Rorc}$ and RAG1KO WT mice after infection.

(D) IL-22 protein quantification secreted by colon explant from non-infected (NI) or infected RAG1KO HIF-1α$^{\Delta Rorc}$ and RAG1KO WT mice cultured for 48 h.

(legend continued on next page)

RORγt$^+$ exhibited no intracellular staining in IL-17. No difference was detected in the absolute number of the different cell subsets on day 5 (Figure 5D). On day 12 of infection, we detected a significant decrease in the percentage of IL-22$^+$ in the Lti and ILC3 subsets (including NKp46$^-$ and NKp46$^+$ ILC3 cells) in the colon of the HIF-1α$^{\Delta Rorc}$ mice compared with the control mice, but not in the non-ILC3 innate RORγt$^+$ IL-22$^+$ cells (Figure 5E). However, no difference was observed in the cell number of the different innate subsets between the WT and HIF-1α$^{\Delta Rorc}$ mice (Figure 5F), suggesting that deficiency of HIF-1α inhibited production of IL-22, as opposed to the expansion or survival of the ILC3s. Furthermore, a significant decrease in the percentage of IL-22$^+$ within the Lti/ILC3 NKp46$^-$ and ILC3 NKp46$^+$ in the colon of the RAG1KO HIF-1α$^{\Delta Rorc}$ mice was also observed compared with the control mice (Figure 5G). No significant variance was observed in the absolute cell count among the various innate subsets on day 12 (Figure 5H). Therefore, the lack of HIF-1α impairs the production of IL-22 by ILC3s following *C. rodentium* infection.

For a detailed investigation of specific ILC3 and ILC1 populations, we performed flow cytometry analysis on RAG1KO HIF-1α$^{\Delta Rorc}$ and control mice on day 12 post-infection. Interestingly, we found a higher percentage of ILC3 NKp46$^-$ subset in RAG1KO HIF-1α$^{\Delta Rorc}$ mice compared with WT mice, despite observing a lower proportion of IL-22$^+$ ILC3s, suggesting a potential compensatory mechanism (Figure S4E). However, there were no observed differences in absolute cell numbers (Figure S4F). Furthermore, the decreased IL-22 production by HIF-1α-deficient ILC3s on day 12 post-infection (Figures 5E and 5G) potentially being attributed to the increased bacterial load and heightened inflammation observed in these transgenic mice was addressed. To eliminate the influence of such environmental secondary factors, IL-22 production was evaluated in colonic ILC3s in response to *C. rodentium* infection in a mixed BM chimera, where both WT and HIF-1α-deficient ILC3s coexist within the same mouse environment. To achieve this, BM from CD45.2 HIF-1α$^{\Delta Rorc}$ mice and their CD45.1 WT littermate controls were transferred into B6 recipient mice. After 12 days of infection, IL-22 was analyzed in the ILC3 CD45.1 WT or ILC3 CD45.2 HIF-1α$^{\Delta Rorc}$ from the colon by flow cytometry, showing that the percentage of IL-22$^+$ cells in ILC3 CD45.2 HIF-1α$^{\Delta Rorc}$ was significantly lower compared with ILC3 CD45.1 WT (Figure S4G).

HIF-1α controls the secretion of IL-22 by ILC3s in response to TLR2 agonist as well as cytokine IL-18

To establish the molecular mechanisms involved in the induction of IL-22 through HIF-1α, we incubated colon explants from the RAG1KO HIF-1α$^{\Delta Rorc}$ mice and the littermate controls with different signals produced by *C. rodentium* infection. As these bacteria are Gram-negative, the innate receptor for bacterial lipopolysaccharide TLR4 could be contributing to the host response.[31] Moreover, TLR2 has been shown to play a critical role in maintaining intestinal mucosal integrity during *C. rodentium* infection.[32] In view of this, we incubated colon explants *in vitro* with LPS (TLR4 agonist) or Pam3CSK4 (TLR2 agonist) for 48 h and IL-22 was then quantified by ELISA. Although IL-22 protein levels did not increase in the supernatant of colon explants from the RAG1KO WT mice stimulated with LPS (Figure 6A), we could detect more IL-22 levels when we stimulated them with Pam3CSK4 and IL-2 (Figure 6B); on the contrary, this enhancement was not observed in stimulated colon explants from the RAG1KO HIF-1α$^{\Delta Rorc}$ mice (Figure 6B), demonstrating that HIF-1α is critical for the induction of IL-22 in ILC3s by TLR2 signaling. Since murine ILC3s do not express TLR2,[33] TLR-induced cytokines were explored as possible activators of HIF-1α-dependent IL-22 production. IL-1β or TL1A combined with IL-23 upregulated IL-22 production in colon explants from both the RAG1KO HIF-1α$^{\Delta Rorc}$ and the WT mice (Figures 6C and 6D), suggesting that HIF-1α was not involved in the induction of IL-22 by ILC3s via these cytokines. However, although IL-18 alone or with IL-23 promoted the secretion of IL-22 by ILC3s from colon explants of the RAG1KO WT mice, this induction was not observed in the RAG1KO HIF-1α$^{\Delta Rorc}$ mice, indicating that IL-18 promoted the secretion of IL-22 through HIF-1α in ILC3s (Figures 6E and 6F). IL-23, TL1A, and IL-2 alone were unable to induce a significant increase in IL-22 when incubated with colon explants from the RAG1KO WT or the RAG1KO HIF-1α$^{\Delta Rorc}$ mice (Figures S5A–S5C).

C. rodentium transcriptionally upregulates HIF-1α in colonic ILC3s to stimulate the production of IL-22 activated by TLR2-induced IL-18

To demonstrate that *C. rodentium* can transcriptionally upregulate HIF-1α and IL-18 in the colon *in vivo*, WT mice were orally infected, and colon RNA was isolated at different time points during the infection for *Hif-1a* and *Il-18* expression quantification. *Hif-1a* mRNA tended to increase over time, with significant upregulation in the colon of infected WT mice at day 12 compared with uninfected ones (Figure 7A). This increase in *Hif-1a* was also observed in sorted colonic ILC3s from WT mice after 12 days of infection, demonstrating transcriptional regulation of HIF-1α in this colonic cell population (Figure 7B). Furthermore, IL-18 was upregulated in the colon of WT mice infected with *C. rodentium*, showing a significant increase after 7 days and maintained up to day 12 of infection (Figure 7C). TLR2 signaling's requirement for IL-18 induction was demonstrated by incubating colon explants from WT mice *ex vivo* with a TLR2 agonist; this led to the production of IL-18 (Figure 7D). An antagonist of IL-18 (IL-18 binding protein; BP IL-18) importantly inhibited IL-22 production induced by TLR2 in colon explants from RAG1KO WT mice, indicating that IL-18, produced upon TLR2 activation, was responsible for inducing IL-22 in colonic ILC3s (Figure 7E).

Significantly, *Hif-1a* mRNA was upregulated in isolated ILC3s from the spleens of WT EGFP$^{+/-}$ control mice when stimulated

(E) Representative images of H&E staining on colon tissues from RAG1KO HIF-1α$^{\Delta Rorc}$ and RAG1KO WT mice on day 12 after *C. rodentium* infection.
(F) Histological score of the colitis inflammation from RAG1KO HIF-1α$^{\Delta Rorc}$ and RAG1KO WT mice 12 days after *C. rodentium* infection. The data represent means ± SD from three independent experiments with n = 7 mice (C and D); from two independent experiments with n = 8 mice (F). Statistical analysis: (A) log rank (Mantel-Cox) test; (B–D) two-way ANOVA with Sidak multiple comparisons; (F) Mann-Whitney U test. *p < 0.05, ***p < 0.001. Symbols represent individual animals.

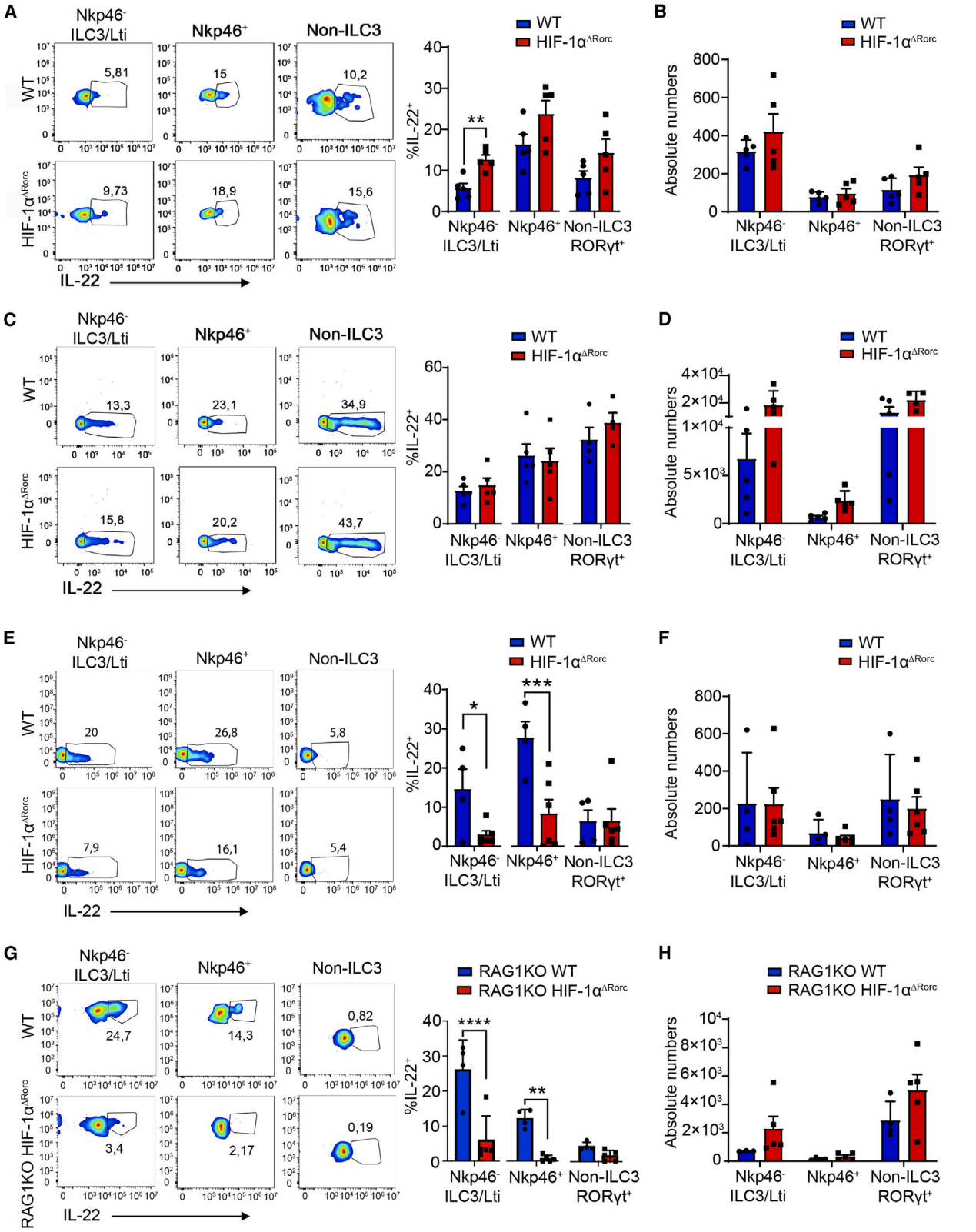

(legend on next page)

in vitro with IL-18 and IL-23 compared with non-stimulated cells (Figure 7F). In addition, the mRNA of glucose transporter 1 (*Slc2a1*), one of the key genes regulated by HIF-1α, was significantly upregulated in these IL-18- and IL-23-stimulated cells (Figure 7G). Importantly, IL-18 alone induced the upregulation of *Hif-1a* in these sorted cells (Figure 7H). Indeed, ILC3s from the spleen of WT EGFP$^{+/-}$ mice significantly upregulated *Il-22* mRNA when stimulated with IL-18 and IL-23 compared with non-stimulated cells. However, this response was not observed in the ILC3s from KO HIF-1α$^{\triangle Rorc}$ EGFP$^{+/-}$ mice (Figure 7I). Notably, there was no difference in *Il-17* mRNA expression in sorted ILC3s from KO HIF-1α$^{\triangle Rorc}$ EGFP$^{+/-}$ mice compared with WT mice when stimulated with IL-18 and IL-23 (Figure 7J). To confirm that IL-22 induction was specific to colonic ILC3s, lamina propria cells from the colon of WT mice were incubated with no stimulus, IL-18 alone, or IL-18 plus IL-23, followed by flow cytometry analysis of intracellular cytokines. ILC3 WT cells significantly upregulated IL-22 after IL-18 induction and even more with IL-18 plus IL-23 (Figure 7K). In contrast, the non-ILC3 innate RORγt$^+$ population did not upregulate IL-22 after IL-18 or IL-18 plus IL-23 stimulation *in vitro* (Figure 7K). These findings demonstrate that HIF-1α is transcriptionally upregulated in colonic ILC3s following *C. rodentium* infection, inducing IL-22 production while not affecting IL-17 in ILC3s via TLR2-induced IL-18.

DISCUSSION

Our research uncovers a pathway for IL-22 production by colonic ILC3s during acute *C. rodentium*-induced colitis. This pathway involves IL-18 upregulation in the colon due to enteric pathogen infection, promoting IL-22 production by colonic ILC3s through HIF-1α. Previously, mTOR1 inhibition (Rptor$^{\triangle Rorc}$ mice, KO of Raptor in the RORγt$^+$ cells) was shown to reduce ILC3 numbers in the small intestine,[34,35] affecting their response to *C. rodentium* infection in the colon, although colonic ILC3 numbers remained unaffected, suggesting other mechanisms at play.[34] Hypoxia boosts ILC3 activation and proliferation, notably observed in the MNK3 cell line.[27] In HIF-1α-deficient RORγt mice, small intestine ILC3 numbers decreased, while ILC1 numbers increased, preserving the RORγt-ILC3 profile.[27] Strikingly, these mice were more susceptible to *Clostridium difficile*, although ILC3s were thought to have a minor role, whereas loss of ILC1s increased susceptibility.[36] Indeed, IL-17-producing γδ T cells, also expressing RORγt, contribute to *C. difficile* protection[37]; consequently, the role of HIF-1α in RORγt$^+$ cells in *C. difficile* susceptibility may involve γδ T cells but requires further investigation. Unlike the HIF-1α-deficient RORγt mice, the loss of HIF-1α, in Nkp46$^+$ cells, prevents ILC3-to-ILC1 conversion, protecting against dextran sodium sulfate colitis-induced intestinal damage.[38]

Herein, we generated transgenic HIF-1α$^{\triangle Rorc}$ mice as an approach for studying the *in vivo* contribution of HIF-1α in RORγt$^+$ cells in the colon. The colonic ILC populations remained stable in steady state, contrasting prior findings in RAG2KO Rptor$^{\Delta Rorc}$ mice.[34] Intriguingly, the absence of *Hif-1a* boosted IL-22 production by ILC3s under steady-state conditions. However, upon *C. rodentium* infection, HIF-1α$^{\triangle Rorc}$ mice exhibited increased susceptibility, likely due to inadequate IL-22 upregulation after 12 days, leading to higher bacterial load and epithelial damage. Surprisingly, IL-17 levels resembled those in WT mice.

Similarly, in RAG1KO HIF-1α$^{\triangle Rorc}$ mice, IL-22 secretion was dysregulated 12 days after *C. rodentium*-induced colitis onset. This resulted in increased susceptibility and severe disease, highlighting the impact of HIF-1α deficiency in innate RORγt$^+$ cells, encompassing ILC3s or other non-ILC3 innate RORγt$^+$ populations. Cytometry analysis revealed that HIF-1α deficiency hindered IL-22 production by ILC3s after 12 days of infection, while other innate RORγt$^+$ cells surprisingly produced IL-22 early during *C. rodentium* infection. Hence, these findings suggest a dual role for HIF-1α in colonic ILC3s, potentially suppressing basal IL-22 production during steady-state conditions and stimulating it during late-stage bacterial infection. Under basal conditions, microbiota-produced butyrate stimulates IL-22 in CD4$^+$ T cells and ILC3s by increasing mTOR, STAT3, AhR, and HIF-1α levels.[35] The findings contradict expectations for HIF-1α$^{\triangle Rorc}$ mice, suggesting that HIF-1α may counteract basal IL-22 secretion in ILC3s through other pathways, for example, involving RANK, VIPR2, or RET.[15,39–44] Further studies are needed for confirmation.

In the late infection stage, we found that HIF-1α regulates IL-22 secretion in colonic ILC3s via IL-18, demonstrated through *ex vivo* experiments using RAG1KO HIF-1α$^{\triangle Rorc}$ mice and their controls. Curiously, previous research showed IL-18-induced HIF-1α *in vitro* in a mouse melanoma cell line.[45] Our study confirms this connection specifically in ILC3s, where *C. rodentium* infection upregulates HIF-1α in colonic tissue and ILC3s, especially when exposed to IL-18 or IL-18 with IL-23. Remarkably, HIF-1α and IL-22 mRNA upregulation in ILC3s occurs after 6 h, indicating direct binding to the IL-22 promoter, similar to CD4$^+$ T cells.[46] This suggests that HIF-1α in ILC3s is regulated by both post-translational changes from hypoxia and an O_2-independent mechanism, as seen in monocytes stimulated with LPS.[47] Moreover, IL-18 was upregulated in *C. rodentium*-infected mice, and

Figure 5. Deficiency of HIF-1α impairs the production of IL-22 by ILC3s

(A and B) Representative flow cytometry dot plots and the percentage of IL-22$^+$ cells (A) in the different innate subsets expressing RORγt (Lti and ILC3 Nkp46$^-$, ILC3 Nkp46$^+$, the non-ILC3 innate RORγt$^+$ cells IL-17R$^-$, CXCR6$^-$, CD90$^-$) or absolute numbers (B) detected in isolated colonic lamina propria cells (LPCs) from the HIF-1α$^{\triangle Rorc}$ and control mice (WT) 2 days after *C. rodentium* infection.

(C and D) Percentage of IL-22$^+$ cells (C) in the different cell populations or absolute numbers (D) after 5 days of *C. rodentium* infection.

(E and F) Percentage of IL-22$^+$ cells (E) in the different subsets or absolute numbers (F) 12 days after *C. rodentium* infection.

(G and H) Percentage of IL-22$^+$ cells (G) in the different populations or absolute numbers (H) in isolated colonic LPC cells from the RAG1KO HIF-1α$^{\triangle Rorc}$ and the control mice RAG1KO WT after 12 days *C. rodentium* infection. Data represent means ± SD from one representative of three independent experiments with n = 5. Statistical analysis: (A, C, E, and G) unpaired t test; (B, D, F, and H) two-way ANOVA with Sidak multiple comparisons. *p < 0.05, **p < 0.01, ***p<0.001, ****p<0,0001. Symbols represent individual animals.

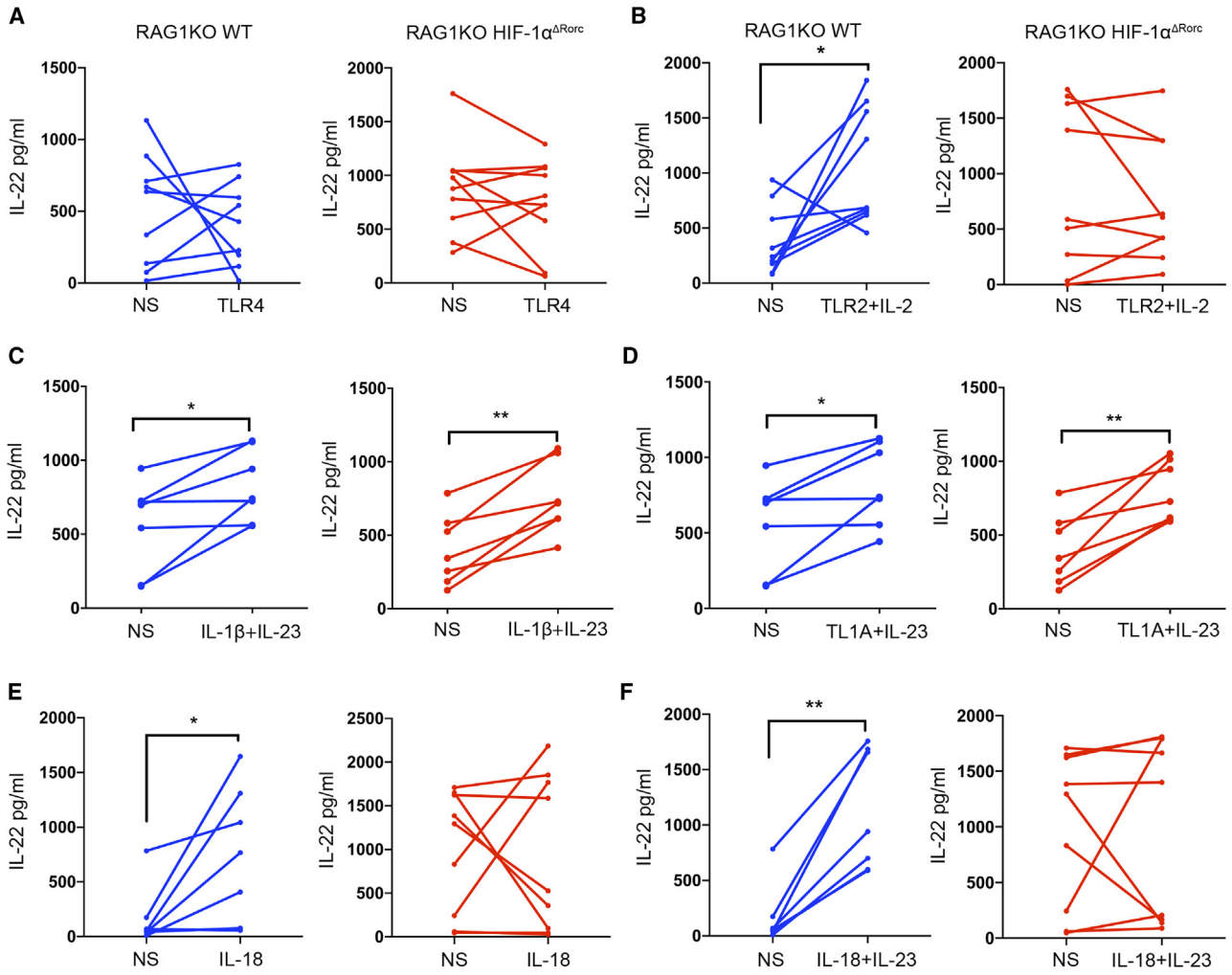

Figure 6. ILC3s release IL-22 in response to TLR2 agonist or IL-18 through HIF-1α

(A) IL-22 protein secretion by colon explants from RAG1KO HIF-1α$^{\Delta Rorc}$ and RAG1KO WT control mice incubated *ex vivo* with TLR4 agonist for 48 h and with non-stimulus (NS).

(B) IL-22 protein secretion by colon explants from RAG1KO HIF-1α$^{\Delta Rorc}$ and RAG1KO WT mice stimulated *ex vivo* with TLR2 agonist and IL-2 for 48 h.

(C) IL-22 protein secretion by colon explants from RAG1KO HIF-1α$^{\Delta Rorc}$ and RAG1KO WT mice incubated *ex vivo* with IL-1β and IL-23 for 48 h.

(D) IL-22 protein secretion by colon explants from RAG1KO HIF-1α$^{\Delta Rorc}$ and RAG1KO WT mice incubated *ex vivo* with TL1A and IL-23 for 48 h.

(E) IL-22 protein secretion by colon explants from RAG1KO HIF-1α$^{\Delta Rorc}$ and RAG1KO WT mice *ex vivo* stimulated with IL-18 for 48 h.

(F) IL-22 protein secretion by colon explants from RAG1KO HIF-1α$^{\Delta Rorc}$ and RAG1KO WT mice incubated *ex vivo* with IL-18 and IL-23 for 48 h. Data representation from three independent experiments with minimum n = 5. Statistical analysis: paired t test. *p < 0.05, **p < 0.01. Symbols represent individual data from one animal with and without stimulus.

it increased IL-22 in WT ILC3s but not in HIF-1α KO ILC3s, while no difference was observed in the upregulation of IL-17, thus demonstrating an independent regulation of both cytokines in this infection model. The highest IL-22 peak occurred on day 12, after the IL-18 peak, indicating the role of IL-18 in IL-22 production in ILC3s. Similar findings were observed during *Toxoplasma gondii* infection in the ileum.[48] Moreover, another study found that human ILC3 proliferation and IL-22 secretion are IL-18 dependent via NF-kB in human tonsils.[49]

Since TLR2 plays an essential role in maintaining mucosal integrity during *C. rodentium*-induced colitis[32] and *C. rodentium* can activate TLR4 in host cells,[31,50] we studied whether the activation of both receptors could induce IL-22 by ILC3s through HIF-1α in colon explants. Our results showed that a TLR2 agonist with IL-2 significantly boosted IL-22 secretion in colon explants from RAG1KO WT mice but not in those from RAG1KO HIF-1α$^{\Delta Rorc}$ mice, suggesting that TLR2 signaling via HIF-1α triggers IL-22 production by ILC3s. Since mouse ILC3s typically lack TLR2 and direct regulation by its ligands,[33] we ruled out direct TLR2 modulation of ILC3s. TLR2 can be expressed by innate and epithelial cells[51] and their activation is associated with IL-18 production.[26,52,53] A defective IL-18 production in IL-18$^{-/-}$ mice causes greater susceptibility to *C. rodentium* infection.[54] During bacterial infections and PAMPs exposure, intestinal epithelial

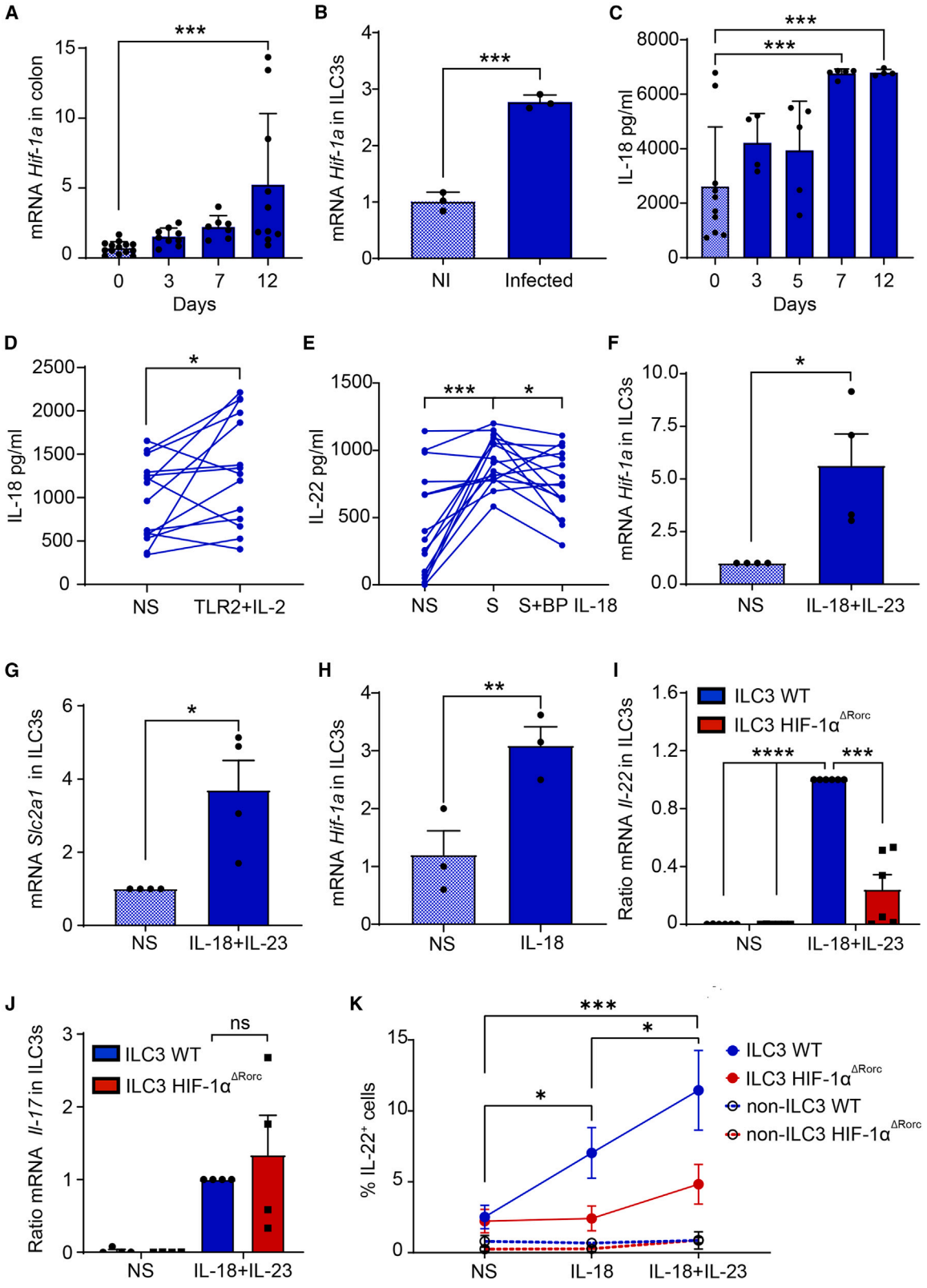

(legend on next page)

cells activate inflammasomes, releasing IL-18.[55] TLR2 stimulation induces proinflammatory cytokines, including IL-18, in human dendritic cells.[53] Our findings indicated that a TLR2 agonist notably promoted IL-18 secretion in colon explants from WT mice. Importantly, an IL-18 antagonist inhibited TLR2-induced IL-22 production in *ex vivo* colon explants from RAG1KO WT mice, suggesting that TLR2-induced IL-18 secretion drives IL-22 production by ILC3s. However, further research is needed to identify the primary source of IL-18 following *C. rodentium* infection in TLR2-dependent signaling.

In summary, we have elucidated a molecular pathway involving TLR2-triggered IL-18 release that transcriptionally regulates HIF-1α expression and IL-22 secretion by ILC3s in the colon during late-stage *C. rodentium* infection. In addition, we observed IL-22 secretion by non-ILC3 innate RORγt$^+$ cells, which, in this context, is independent of HIF-1α expression. These findings hold promise for advancing research in colitis, enteropathogen infections, IBDs, and cancer progression.

Limitations of the study

Regrettably, this study could not ascertain the production of IL-22 in the different subsets of sorted RORγt$^+$ cells from the colon of infected mice, primarily due to technical intricacies. Interestingly, further exploration is needed to analyze the role of the characterized non-ILC3 innate RORγt$^+$ cells in the control of the *C. rodentium* infection.

STAR★METHODS

Detailed methods are provided in the online version of this paper and include the following:

- KEY RESOURCES TABLE
- RESOURCE AVAILABILITY
  - Lead contact
  - Materials availability
  - Data and code availability
- EXPERIMENTAL MODEL AND STUDY PARTICIPANT DETAILS
  - Mice
  - BM chimeras
  - Citrobacter rodentium-induced colitis
- METHOD DETAILS
  - Counting of colonic patches
  - Isolation of colonic LPCs
  - Flow cytometry, antibodies, and ELISA
  - Flow cytometry gating strategy
  - *Ex vivo* organ culture
  - Isolation of splenic ILC3s
  - Histology
  - Immunofluorescence
  - RNA isolation and qPCR
- QUANTIFICATION AND STATISTICAL ANALYSIS

SUPPLEMENTAL INFORMATION

Supplemental information can be found online at https://doi.org/10.1016/j.celrep.2023.113508.

ACKNOWLEDGMENTS

The authors wish to thank the Flow Cytometry Core Facility of the CBMSO and the CIB, the Histology and Microscopy Facilities of CNB, and the Genomic Facility of CAI at UCM and "Parque Científico de Madrid" for the technical support provided. The graphical abstract was created using Biorender software. The present research was supported by the "Ramon y Cajal'' Program (RYC-2017-21837), the grant nos. RTI2018-093647-B-I00, CNS2022-135365, and PID2021-122780OB-I00 awarded to A.C.-A. by the "Ministerio de Ciencia e Innovación", Agencia Estatal de Investigación (AEI). JMGG's laboratory is supported by grants from the Instituto de Salud Carlos III (ISCIII) (PI20/00306). All these grants were co-funded by the European Regional Development Fund (ERDF) "A way to build Europe". A.V.-N. is a recipient of an FPI fellowship (PRE2019-090341) from the "Ministerio de Ciencia e Innovación." R.C.-G. is a recipient of a Juan de la Cierva grant (FJC2021-047282-I) from the Ministerio de Ciencia e Innovación. C.V.-G. is supported by "Programa Investigo Comunidad de Madrid" (09-PIN1-00009.8/2022) and L.S.-T. is supported by the PID2021-122780OB-I00 project by the "Ministerio de Ciencia e Innovación." Currently, L.S.-T. has been awarded an FPU grant (FPU22/02155) from the "Ministerio de Educación y Formación Profesional."

AUTHOR CONTRIBUTIONS

A.V.-N. performed and analyzed most of the experiments and helped to draft the manuscript. M.J.G.-S. performed experiments and analyzed some of the data. L.S.-T., C.V.-G., and R.C.-G. performed experiments, designed the figures, and revised the manuscript. A.O.-R. performed some of the colon explant experiments. B.S.P. analyzed the localization of ILCs by means of a confocal analysis. V.Z. performed the experiments of the BM chimeras.

Figure 7. *C. rodentium* infection causes TLR2-induced IL-18 production in the colon, which transcriptionally upregulates *Hif-1a* in ILC3s, promoting IL-22 expression

(A) Gene expression of *Hif-1a* in the colon from uninfected and infected WT mice after 3, 7, and 12 days.
(B) *Hif-1a* relative expression in sorted ILC3s from WT mice non-infected (NI) and after 12 days infection.
(C) IL-18 protein secretion by colon explants from the uninfected and *C. rodentium*-infected WT mice after 3, 5, 7, and 12 days.
(D) IL-18 protein secretion by colon explants from WT mice incubated *ex vivo* with IL-2 and TLR2 agonist (Pam3CSK4) for 24 h and with non-stimulus (NS).
(E) IL-22 protein secretion by colon explants from RAG1KO WT mice incubated for 48 h ex *vivo* with Pam3CSK4 and IL-2 (S, stimulus) and blocked with the BP IL-18 (S + BP IL-18).
(F and G) Gene expression of *Hif-1a* (F) or *Slc2a1* (G) in sorted ILC3s from the spleen of WT EGFP$^{+/-}$ mice incubated *ex vivo* with or without IL-18 and IL-23 for 6 h.
(H) Gene expression of *Hif-1a* in sorted splenic ILC3s of WT EGFP$^{+/-}$ *ex vivo* incubated with or without IL-18 for 6 h.
(I and J) Gene expression of *Il-22* (I) or *Il-17* (J) in sorted splenic ILC3s of the WT EGFP$^{+/-}$ and HIF-1$\alpha^{\triangle Rorc}$ EGFP$^{+/-}$ mice incubated *ex vivo* with or without IL-18 and IL-23 for 6 h. The levels of mRNA are normalized to the stimulated WT.
(K) Percentage of IL-22$^+$ cells in ILC3s or in the non-ILC3 innate RORγt$^+$ subsets of LPCs from HIF-1$\alpha^{\triangle Rorc}$ or WT mice, unstimulated (NS) or incubated *ex vivo* with IL-18 or IL-18 plus IL-23 overnight, quantified by flow cytometry. Statistically significant when comparing unstimulated ILC3 WT cells with stimulation. Data represent the means ± SD from three (A, B, and H–J), two (C, K, and L), or four (D–G) independent experiments. Statistical analysis: (A and B) unpaired t test; (D and F–H) paired t test; (E, K, and L) RM one-way ANOVA test; (C, I, and J) one-way ANOVA with Sidak multiple comparisons. n.s., not significant; *p < 0.05, **p < 0.01, ***p < 0.001.

B.R.-P. analyzed the ILC populations in the colon using the dimensionality reduction algorithm and assisted in the multi-parameter setting. P.Y.-F. helped in the sorting of ILC3s and the multiparametric analysis using the Cytoflex cytometer. J.M.G.-G. provided some protocols, expertise, and reagents. J.A. provided the HIF-1$\alpha^{fl/fl}$ Ub-Cre ERT2 mice for the BM chimera experiments and reviewed the manuscript. A.C.-A. conceptualized the study, designed, supervised, analyzed the experiments, and wrote the manuscript. All authors contributed to the article and approved the submitted version.

DECLARATION OF INTERESTS

The authors declare no competing interests.

Received: April 18, 2023
Revised: October 24, 2023
Accepted: November 13, 2023
Published: November 28, 2023

REFERENCES

1. Petri, W.A., Miller, M., Binder, H.J., Levine, M.M., Dillingham, R., and Guerrant, R.L. (2008). Enteric infections, diarrhea, and their impact on function and development. J. Clin. Invest. *118*, 1277–1290.
2. Croxen, M.A., Law, R.J., Scholz, R., Keeney, K.M., Wlodarska, M., and Finlay, B.B. (2013). Recent advances in understanding enteric pathogenic Escherichia coli. Clin. Microbiol. Rev. *26*, 822–880.
3. Bouladoux, N., Harrison, O.J., and Belkaid, Y. (2017). The Mouse Model of Infection with Citrobacter rodentium. Curr. Protoc. Immunol. *119*, 19.
4. Collins, J.W., Keeney, K.M., Crepin, V.F., Rathinam, V.A.K., Fitzgerald, K.A., Finlay, B.B., and Frankel, G. (2014). Citrobacter rodentium: Infection, inflammation and the microbiota. Nat. Rev. Microbiol. *12*, 612–623.
5. Mundy, R., MacDonald, T.T., Dougan, G., Frankel, G., and Wiles, S. (2005). Citrobacter rodentium of mice and man. Cell Microbiol. *7*, 1697–1706.
6. Cruz-Adalia, A., and Veiga, E. (2016). Close encounters of lymphoid cells and bacteria. Front. Immunol. *7*, 405.
7. Vivier, E., Artis, D., Colonna, M., Diefenbach, A., di Santo, J.P., Eberl, G., Koyasu, S., Locksley, R.M., McKenzie, A.N.J., Mebius, R.E., et al. (2018). Innate Lymphoid Cells: 10 Years On. Cell *174*, 1054–1066.
8. Domingues, R.G., and Hepworth, M.R. (2020). Immunoregulatory Sensory Circuits in Group 3 Innate Lymphoid Cell (ILC3) Function and Tissue Homeostasis. Front. Immunol. *11*, 116.
9. Eberl, G., Marmon, S., Sunshine, M.-J., Rennert, P.D., Choi, Y., and Littman, D.R. (2004). An essential function for the nuclear receptor RORγt in the generation of fetal lymphoid tissue inducer cells. Nat. Immunol. *5*, 64–73.
10. Luci, C., Reynders, A., Ivanov, I.I., Cognet, C., Chiche, L., Chasson, L., Hardwigsen, J., Anguiano, E., Banchereau, J., Chaussabel, D., et al. (2009). Influence of the transcription factor RORγt on the development of NKp46+ cell populations in gut and skin. Nat. Immunol. *10*, 75–82.
11. Satoh-Takayama, N., Vosshenrich, C.A.J., Lesjean-Pottier, S., Sawa, S., Lochner, M., Rattis, F., Mention, J.-J., Thiam, K., Cerf-Bensussan, N., Mandelboim, O., et al. (2008). Microbial Flora Drives Interleukin 22 Production in Intestinal NKp46+ Cells that Provide Innate Mucosal Immune Defense. Immunity *29*, 958–970.
12. Sonnenberg, G.F., Monticelli, L.A., Elloso, M.M., Fouser, L.A., and Artis, D. (2011). CD4(+) lymphoid tissue-inducer cells promote innate immunity in the gut. Immunity *34*, 122–134.
13. Qiu, J., Heller, J.J., Guo, X., Chen, Z.M.E., Fish, K., Fu, Y.X., and Zhou, L. (2012). The Aryl Hydrocarbon Receptor Regulates Gut Immunity through Modulation of Innate Lymphoid Cells. Immunity *36*, 92–104.
14. Guo, X., Qiu, J., Tu, T., Yang, X., Deng, L., Anders, R.A., Zhou, L., and Fu, Y.X. (2014). Induction of innate lymphoid cell-derived interleukin-22 by the transcription factor STAT3 mediates protection against intestinal infection. Immunity *40*, 25–39.
15. Valle-Noguera, A., Ochoa-Ramos, A., Gomez-Sánchez, M.J., and Cruz-Adalia, A. (2021). Type 3 Innate Lymphoid Cells as Regulators of the Host-Pathogen Interaction. Front. Immunol. *12*, 748851.
16. Zheng, Y., Valdez, P.A., Danilenko, D.M., Hu, Y., Sa, S.M., Gong, Q., Abbas, A.R., Modrusan, Z., Ghilardi, N., de Sauvage, F.J., and Ouyang, W. (2008). Interleukin-22 mediates early host defense against attaching and effacing bacterial pathogens. Nat. Med. *14*, 282–289.
17. Iique Jarade, A., Di Santo, J.P., and Serafini, N. (2021). Group 3 innate lymphoid cells mediate host defense against attaching and effacing pathogens. Curr. Opin. Microbiol. *63*, 83–91.
18. Cella, M., Fuchs, A., Vermi, W., Facchetti, F., Otero, K., Lennerz, J.K.M., Doherty, J.M., Mills, J.C., and Colonna, M. (2009). A human natural killer cell subset provides an innate source of IL-22 for mucosal immunity. Nature *457*, 722–725.
19. Castellanos, J.G., Woo, V., Viladomiu, M., Putzel, G., Lima, S., Diehl, G.E., Marderstein, A.R., Gandara, J., Perez, A.R., Withers, D.R., et al. (2018). Microbiota-induced TNF-like ligand 1A drives group 3 innate lymphoid cell-mediated barrier protection and intestinal T cell activation during colitis. Immunity *49*, 1077–1089.e5.
20. Lyu, M., Suzuki, H., Kang, L., Gaspal, F., Zhou, W., Goc, J., Zhou, L., Zhou, J., Zhang, W., et al.; JRI Live Cell Bank (2022). ILC3s select microbiota-specific regulatory T cells to establish tolerance in the gut. Nature *610*, 744–751.
21. Kedmi, R., Najar, T.A., Mesa, K.R., Grayson, A., Kroehling, L., Hao, Y., Hao, S., Pokrovskii, M., Xu, M., Talbot, J., et al. (2022). A RORγt+ cell instructs gut microbiota-specific Treg cell differentiation. Nature *610*, 737–743.
22. Akagbosu, B., Tayyebi, Z., Shibu, G., Paucar Iza, Y.A., Deep, D., Parisotto, Y.F., Fisher, L., Pasolli, H.A., Thevin, V., Elmentaite, R., et al. (2022). Novel antigen-presenting cell imparts Treg-dependent tolerance to gut microbiota. Nature *610*, 752–760.
23. Yamano, T., Dobeš, J., Vobořil, M., Steinert, M., Brabec, T., Ziętara, N., Dobešová, M., Ohnmacht, C., Laan, M., Peterson, P., et al. (2019). Aire-expressing ILC3-like cells in the lymph node display potent APC features. J. Exp. Med. *216*, 1027–1037.
24. Sonnenberg, G.F., and Artis, D. (2015). Innate lymphoid cells in the initiation, regulation and resolution of inflammation. Nat. Med. *21*, 698–708.
25. Castellanos, J.G., and Longman, R.S. (2020). Innate lymphoid cells link gut microbes with mucosal T cell immunity. Gut Microb. *11*, 231–236.
26. Muñoz, M., Eidenschenk, C., Ota, N., Wong, K., Lohmann, U., Kühl, A.A., Wang, X., Manzanillo, P., Li, Y., Rutz, S., et al. (2015). Interleukin-22 Induces Interleukin-18 Expression from Epithelial Cells during Intestinal Infection. Immunity *42*, 321–331.
27. Fachi, J.L., Pral, L.P., dos Santos, J.A.C., Codo, A.C., de Oliveira, S., Felipe, J.S., Zambom, F.F.F., Câmara, N.O.S., Vieira, P.M.M.M., Colonna, M., and Vinolo, M.A.R. (2021). Hypoxia enhances ILC3 responses through HIF-1α-dependent mechanism. Mucosal Immunol. *14*, 828–841.
28. Palazon, A., Goldrath, A.W., Nizet, V., and Johnson, R.S. (2014). HIF transcription factors, inflammation, and immunity. Immunity *41*, 518–528.
29. Glover, L.E., and Colgan, S.P. (2011). Hypoxia and metabolic factors that influence inflammatory bowel disease pathogenesis. Gastroenterology *140*, 1748–1755.
30. Honda, K. (2012). IL-22 from T Cells: Better Late than Never. Immunity *37*, 952–954.
31. Khan, M.A., Ma, C., Knodler, L.A., Valdez, Y., Rosenberger, C.M., Deng, W., Finlay, B.B., and Vallance, B.A. (2006). Toll-Like Receptor 4 Contributes to Colitis Development but Not to Host Defense during Citrobacter rodentium Infection in Mice. Infect. Immun. *74*, 2522–2536.
32. Gibson, D.L., Ma, C., Rosenberger, C.M., Bergstrom, K.S.B., Valdez, Y., Huang, J.T., Khan, M.A., and Vallance, B.A. (2008). Toll-like receptor 2 plays a critical role in maintaining mucosal integrity during Citrobacter rodentium-induced colitis. Cell Microbiol. *10*, 388–403.

33. Crellin, N.K., Trifari, S., Kaplan, C.D., Satoh-Takayama, N., Di Santo, J.P., and Spits, H. (2010). Regulation of Cytokine Secretion in Human CD127+ LTi-like Innate Lymphoid Cells by Toll-like Receptor 2. Immunity *33*, 752–764.

34. Teufel, C., Horvath, E., Peter, A., Ercan, C., Piscuoglio, S., Hall, M.N., Finke, D., and Lehmann, F.M. (2021). mTOR signaling mediates ILC3-driven immunopathology. Mucosal Immunol. *14*, 1323–1334.

35. Di Luccia, B., Gilfillan, S., Cella, M., Colonna, M., and Huang, S.C.C. (2019). ILC3s integrate glycolysis and mitochondrial production of reactive oxygen species to fulfill activation demands. J. Exp. Med. *216*, 2231–2241.

36. Abt, M.C., Lewis, B.B., Caballero, S., Xiong, H., Carter, R.A., Sušac, B., Ling, L., Leiner, I., and Pamer, E.G. (2015). Innate immune defenses mediated by two ilc subsets are critical for protection against acute clostridium difficile infection. Cell Host Microbe *18*, 27–37.

37. Chen, Y.S., Chen, I.B., Pham, G., Shao, T.Y., Bangar, H., Way, S.S., and Haslam, D.B. (2020). IL-17–producing γδ T cells protect against Clostridium difficile infection. J. Clin. Invest. *130*, 2377–2390.

38. Krzywinska, E., Sobecki, M., Nagarajan, S., Zacharjasz, J., Tambuwala, M.M., Pelletier, A., Cummins, E., Gotthardt, D., Fandrey, J., Kerdiles, Y.M., et al. (2022). The transcription factor HIF-1α mediates plasticity of NKp46+ innate lymphoid cells in the gut. J. Exp. Med. *219*, e20210909.

39. Seillet, C., Luong, K., Tellier, J., Jacquelot, N., Shen, R.D., Hickey, P., Wimmer, V.C., Whitehead, L., Rogers, K., Smyth, G.K., et al. (2020). The neuropeptide VIP confers anticipatory mucosal immunity by regulating ILC3 activity. Nat. Immunol. *21*, 168–177.

40. Talbot, J., Hahn, P., Kroehling, L., Nguyen, H., Li, D., and Littman, D.R. (2020). Feeding-dependent VIP neuron–ILC3 circuit regulates the intestinal barrier. Nature *579*, 575–580.

41. Pascal, M., Kazakov, A., Chevalier, G., Dubrule, L., Deyrat, J., Dupin, A., Saha, S., Jagot, F., Sailor, K., Dulauroy, S., et al. (2022). The neuropeptide VIP potentiates intestinal innate type 2 and type 3 immunity in response to feeding. Mucosal Immunol. *15*, 629–641.

42. Yu, H.B., Yang, H., Allaire, J.M., Ma, C., Graef, F.A., Mortha, A., Liang, Q., Bosman, E.S., Reid, G.S., Waschek, J.A., et al. (2021). Vasoactive intestinal peptide promotes host defense against enteric pathogens by modulating the recruitment of group 3 innate lymphoid cells. Proc Natl Acad Sci USA *118*, e2106634118.

43. Ibiza, S., García-Cassani, B., Ribeiro, H., Carvalho, T., Almeida, L., Marques, R., Misic, A.M., Bartow-McKenney, C., Larson, D.M., Pavan, W.J., et al. (2016). Glial-cell-derived neuroregulators control type 3 innate lymphoid cells and gut defence IL-22. Nature *535*, 440–443.

44. Bando, J.K., Gilfillan, S., Song, C., McDonald, K.G., Huang, S.C.C., Newberry, R.D., Kobayashi, Y., Allan, D.S.J., Carlyle, J.R., Cella, M., and Colonna, M. (2018). The Tumor Necrosis Factor Superfamily Member RANKL Suppresses Effector Cytokine Production in Group 3 Innate Lymphoid Cells Graphical Abstract Highlights d CCR6 + ILC3s from Rorc Cre Tnfsf11 fl/fl mice have enhanced IL-17A and IL-22 production d Loss of Tnfsf11 in ILC3s, and not T cells, leads to hyperresponsive CCR6 + ILC3s d RANKL directly suppresses ILC3s via RANK, and RANK deficiency enhances ILC3 activity d CCR6 + ILC3s lacking RANKL have increased amounts of RORgt. Immunity *48*, 1208–1219.e4.

45. Kim, J., Shao, Y., Kim, S.Y., Kim, S., Song, H.K., Jeon, J.H., Suh, H.W., Chung, J.W., Yoon, S.R., Kim, Y.S., and Choi, I. (2008). Hypoxia-induced IL-18 Increases Hypoxia-inducible Factor-1 Expression through a Rac1-dependent NF-B Pathway. Mol. Biol. Cell *19*, 433–444.

46. Budda, S.A., Girton, A., Henderson, J.G., and Zenewicz, L.A. (2016). Transcription Factor HIF-1α Controls Expression of the Cytokine IL-22 in CD4 T Cells. J. Immunol. *197*, 2646–2652.

47. Frede, S., Stockmann, C., Freitag, P., and Fandrey, J. (2006). Bacterial lipopolysaccharide induces HIF-1 activation in human monocytes via p44/42 MAPK and NF-κB. Biochem. J. *396*, 517–527.

48. Couturier-Maillard, A., Froux, N., Piotet-Morin, J., Michaudel, C., Brault, L., Le Bérichel, J., Sénéchal, A., Robinet, P., Chenuet, P., Jejou, S., et al. (2018). Interleukin-22-deficiency and microbiota contribute to the exacerbation of Toxoplasma gondii-induced intestinal inflammation article. Mucosal Immunol. *11*, 1181–1190.

49. Victor, A.R., Nalin, A.P., Dong, W., McClory, S., Wei, M., Mao, C., Kladney, R.D., Youssef, Y., Chan, W.K., Briercheck, E.L., et al. (2017). IL-18 Drives ILC3 Proliferation and Promotes IL-22 Production via NF-kB. J. Immunol. *199*, 2333–2342.

50. Ji, Q., Zhang, Y., Zhou, Y., Gamah, M., Yuan, Z., Liu, J., Cao, C., Gao, X., Zhang, H., Ren, Y., and Zhang, W. (2020). Effects of hypoxic exposure on immune responses of intestinal mucosa to Citrobacter colitis in mice. Biomed. Pharmacother. *129*, 110477.

51. Burgueño, J.F., and Abreu, M.T. (2020). Epithelial Toll-like receptors and their role in gut homeostasis and disease. Nat. Rev. Gastroenterol. Hepatol. *17*, 263–278.

52. Fukata, M., and Arditi, M. (2013). The role of pattern recognition receptors in intestinal inflammation. Mucosal Immunol. *6*, 451–463.

53. Re, F., and Strominger, J.L. (2001). Toll-like Receptor 2 (TLR2) and TLR4 Differentially Activate Human Dendritic Cells. J. Biol. Chem. *276*, 37692–37699.

54. Liu, Z., Zaki, M.H., Vogel, P., Gurung, P., Finlay, B.B., Deng, W., Lamkanfi, M., and Kanneganti, T.D. (2012). Role of Inflammasomes in Host Defense against Citrobacter rodentium Infection. J. Biol. Chem. *287*, 16955–16964.

55. Lei-Leston, A.C., Murphy, A.G., and Maloy, K.J. (2017). Epithelial cell inflammasomes in intestinal immunity and inflammation. Front. Immunol. *8*, 1168.

56. Tumanov, A.V., Koroleva, E.P., Guo, X., Wang, Y., Kruglov, A., Nedospasov, S., and Fu, Y.-X. (2011). Lymphotoxin Controls the IL-22 Protection Pathway in Gut Innate Lymphoid Cells during Mucosal Pathogen Challenge. Cell Host Microbe *10*, 44–53.

57. Wang, Y., Koroleva, E.P., Kruglov, A.A., Kuprash, D.v., Nedospasov, S.A., Fu, Y.-X., and Tumanov, A.v. (2010). Lymphotoxin Beta Receptor Signaling in Intestinal Epithelial Cells Orchestrates Innate Immune Responses against Mucosal Bacterial Infection. Immunity *32*, 403–413.

58. Rankin, L.C., Girard-Madoux, M.J.H., Seillet, C., Mielke, L.A., Kerdiles, Y., Fenis, A., Wieduwild, E., Putoczki, T., Mondot, S., Lantz, O., et al. (2016). Complementarity and redundancy of IL-22-producing innate lymphoid cells. Nat. Immunol. *17*, 179–186.

59. Valle-Noguera, A., Gómez-Sánchez, M.J., Girard-Madoux, M.J.H., and Cruz-Adalia, A. (2020). Optimized Protocol for Characterization of Mouse Gut Innate Lymphoid Cells. Front. Immunol. *11*, 563414.

60. Wu, X., Vallance, B.A., Boyer, L., Bergstrom, K.S.B., Walker, J., Madsen, K., O'Kusky, J.R., Buchan, A.M., and Jacobson, K. (2008). Saccharomyces boulardii ameliorates Citrobacter rodentium-induced colitis through actions on bacterial virulence factors. Am. J. Physiol. Gastrointest. Liver Physiol. *294*, 295–306.

STAR★METHODS

KEY RESOURCES TABLE

REAGENT or RESOURCE	SOURCE	IDENTIFIER
Antibodies		
CD45.2 PerCP-Cy 5.5 Mouse anti-mouse Clon:104	BD Biosciences	RRID: AB_394528
CD127 Anti-Mouse PE Cy-5 Clone: A7R34	Thermo Fisher Scientific	RRID: AB_468792
CD335 (Nkp46) Anti-mouse PE-Cyanine7 Clone: 2941.4	Thermo Fisher Scientific	RRID: AB_2573442
CD4 anti-mouse FITC Clone: GK1.5 CD4 anti-mouse Alexa Fluor 700	TONBO biosciences Thermo Fisher Scientific	RRID: AB2621665 RRID: AB_493999
CD90.2 anti-mouse BV650 Clone: 53–2.1	BD Biosciences	RRID: AB_2740170
KLRG1 Anti - Mouse APC-eFLUOR 780 Clon: 2F1	Thermo Fisher Scientific	RRID: AB_2573988
CD3 Anti-mouse APC/Cyanine7 Clone: 17A2 Isotype: Rat IgG2b CD3 Anti-mouse PE-Cyanine 5 Clone: 145-2C11	Biolegend TONBO biosciences	RRID: AB_2242784 RRID: AB_2621815
CD19 Anti-mouse FITC Clone: 1D3	TONBO biosciences	RRID: AB_2621682
CD5 anti-mouse BV421 Clone: 53–7.3	Biolegend	RRID: AB_2562173
CCR6 anti-mouse APC Clone:29-2L17	Biolegend	RRID: AB_1877147
CXCR6 Anti-mouse PE/Cyanine7 Clone: SA051D1	Biolegend	RRID: AB_2721670
Ly-6G and Ly-6C (GR-1) Rat anti-mouse BV421 Clone: RB6-8C5	BD Biosciences	RRID: AB_2737736
F4/80 Rat anti-mouse BV421 Clone: T45-2342	BD Biosciences	RRID: AB_2734779
GATA-3 Alexa Fluor 488 Mouse Clone: L50-823 GATA-3 Mouse BV421 Clone: L50-823	BD Biosciences BD Biosciences	RRID: AB_1645302 RRID: AB_2738152
RORγt Mouse/Anti-Mouse BV421 RORγt Anti-Hu/Mo PE	BD Biosciences Invitrogen	RRID: AB_2687545 RRID: AB_1834470
EOMES Anti-Mouse PE-eFluor 610 Clone: Dan11mag	Thermo Fisher Scientific	RRID: AB_2574613
CD16/CD32 (Fc block) Clone. 2.4G2	BD Biosciences	RRID: AB_394656
IL-22 anti-mouse PE Clone: 1H8PWSR	Thermo Fisher Scientific	RRID: AB_10597428
IL7R anti-mouse/rat PE/Cyanine5 Clone: A7R34	Biolegend	RRID: AB_1937261
IL-17A Anti- Mouse/Rat APC Clone: eBio17B7	Thermo Fisher Scientific	RRID: AB_763580
TCRβ anti-mouse BV421 Clone: H57-597	Biolegend	RRID: AB_10933263
TCRγδ anti-mouse BV421 Clone: GL3	Biolegend	RRID: AB_10896753
Rat IgG2a Isotype control Clone: 2A3	BioXcell	RRID: AB_1107769
Mouse anti-GFP	Roche Applied Science. Sigma-Aldrich	RRID:AB_390913
Goat anti-Mouse Alexa 488	Thermo Fisher Scientific	RRID: AB_2534088
CD3 Monoclonal Antibody (17A2)	Thermo Fisher Scientific	RRID: AB_467053
CD3 antibody	Abcam	RRID: AB_305055
B220 anti-mouse Clone: RA3-6B2	StemCell	100–0422
Goat anti-Rat Alexa 647	Thermo Fisher Scientific	RRID: AB_141778
Goat anti-rabbit Cy3	Jackson ImmunoResearch	RRID: AB_2338009
Chemicals, peptides, and recombinant proteins		
Recombinant mouse IL-23 protein (Sf21-derived) Lot DFXU0720061 > 95% purity	R&D	1887-ML
Recombinant mouse IL-1β protein 1	Stem Cell	78035.1
Recombinant mouse IL-18 protein 10ug (E-coli derived)	R&D	9139–IL/CF
Recombinant mouse TL1A protein Recombinant Mouse TNFSF15 (carrier-free) 10ug	Biolegend	753002
Pam3CSK4 1mg	TOCRIS	4633/1

(*Continued on next page*)

Continued

REAGENT or RESOURCE	SOURCE	IDENTIFIER
Lipopolysaccharides from *Escherichia Coli* O111:B4 (LPS)	Sigma-Aldrich	L2630
Brefeldin A	Cell signaling	9972S
Stop Golgi	BD Biosciences	554724
BlockAidTM Blocking Solution	Life technologies	B10710
ProLong mounting medium	ThermoFisher Scientific	P36984
MacConkey agar	Oxoid	CM007B
Sodium thiosulfate	Sigma Aldrich	1.065.122.500
Ammonium citrate	Sigma Aldrich	RES20400-A7
TRIzol	Sigma Aldrich	T9424
PCR Power SYBR Green	Applied Biosystems	4367659
DAPI	Sigma Aldrich	32670
EvaGreen® qPCR Mix Plus ROX	Solis Biodyne	08-24-0000S
Critical commercial assays		
Foxp3/Transcription Factor Staining Buffer Set	Thermo Fisher Scientific	00-5523-00
ELISA IL-18 Mouse Uncoated kit	Thermo Fisher Scientific	88-50618-88
ELISA IL-22 10 × 96 Tests	Thermo Fisher Scientific	88-7422-88
ELISA IL-17 Mouse Uncoated kit	Thermo Fisher Scientific	88-8711-88
RNeasy Micro Kit	Qiagen	74004
MojoSort^{TM} Mouse CD4 T cell Isolation Kit	Biolegend	480033
Experimental models: Organisms/strains		
B6-SJL (Ptprc^{a} Pepc^{b}/BoyJ) expressing CD45.1 allele	Jackson Laboratory	#:002014 RRID:IMSR_JAX:002014
B6.129-*Hif1a*^{tm3Rsjo}/J (HIF1α^{flox})	Aragones J's laboratory- from Jackson Laboratory	#:007561 RRID:IMSR_JAX:007561
HIF-1$\alpha^{fl/fl}$ Ub-Cre ERT2	Aragones J's laboratory	
B6.Cg-*Ndor1*$^{Tg(UBC-cre/ERT2)1Ejb}$/1J (WT Ub-Cre ERT2)	Aragones J's laboratory- from Jackson Laboratory	#:007561 RRID:IMSR_JAX:007001
B6.FVB-Tg(Rorc-cre)1Litt/J (RORγtCre mice)	Jackson Laboratory	#:022791 RRID:IMSR_JAX:022791
B6.129P2(Cg)-*Rorc*^{tm2Litt}/J (RORγt EGFP mice)	Jackson Laboratory	#:007572 RRID:IMSR_JAX:007572
HIF-1$\alpha^{fl/fl}$ RORγtCre (HIF-1$\alpha^{\triangle Rorc}$)	This paper	N/A
B6.129S7-*Rag1*^{tm1Mom}/J (RAG1KO)	Veiga E's laboratory from Jackson Laboratory	#:002216 RRID:IMSR_JAX:002216
RAG1KO HIF-1$\alpha^{fl/fl}$ RORγtCre (RAG1KO HIF-1$\alpha^{\triangle Rorc}$)	This paper	N/A
HIF-1$\alpha^{fl/fl}$ RORγtCre EGFP (HIF-1$\alpha^{\triangle Rorc}$ EGFP$^{+/-}$)	This paper	N/A
Software and algorithms		
CytExpert software	Beckham Coulter	RRID:SCR_017217
Flowjo software	BD Biosciences	RRID:SCR_008520
GraphPad Prism software	Dotmatics	RRID:SCR_002798
OMIQ software	Dotmatics	N/A
Biorender software	Biorender	RRID:SCR_018361
Fiji	Open Source	RRID: SCR_002285

RESOURCE AVAILABILITY

Lead contact

Further information and requests for resources and reagents should be directed to, and will be addressed by, the Lead Contact, Cruz-Adalia A (arancruz@ucm.es).

Materials availability

The mouse lines generated in the present study will be made available on request by the Lead Contact without restriction.

Data and code availability

- All original data reported in this paper are available from the lead contact upon request.
- This paper does not report original code.
- Any additional information required to reanalyze the data reported in this paper is available from the lead contact upon request.

EXPERIMENTAL MODEL AND STUDY PARTICIPANT DETAILS

Mice

HIF-1$\alpha^{fl/fl}$RORγtCre (HIF-1$\alpha^{\triangle Rorc}$) mice were generated by crossing B6.129-Hif1αtm3Rsjo/J mice with B6.Cg-Ndor1Tg(UBC-cre/ERT2)1Ejb/1J mice. The *Rorc*gfp/+ mice[9] were crossed with HIF-1$\alpha^{\triangle Rorc}$ to generate the HIF-1$\alpha^{\triangle Rorc}$ EGFP$^{+/-}$ mice. RAG1KO mice were crossed with HIF-1$\alpha^{\triangle Rorc}$ mice to generate the RAG1KO HIF-1$\alpha^{\triangle Rorc}$ mice. The *Hif-1a*floxed-UBC-Cre-ERT2 mice were generated by crossing B6.129-*Hif1a*tm3Rsjo/J mice with B6.Cg-Ndor1Tg(UBC-cre/ERT2)1Ejb/1J mice, which harbor two *loxP* sites flanking exon 2 of the murine *Hif-1a* and B6.Tg (UBC-Cre/ERT2) mice, which ubiquitously express a tamoxifen-inducible CRE recombinase (Cre-ERT2). The *Hif-1a*floxed-UBC-Cre-ERT2mice were kindly provided by our collaborator Dr. Julián Aragonés (UAM). For *Hif-1a* gene inactivation, the mice were given *ad libitum* access to Teklad CRD TAM400/CreER tamoxifen pellets (The Harlan Laboratory) for 10–15 days or an intraperitoneal injection of 100 μL (20 mg/mL) tamoxifen for 5 days followed by standard mouse chow diet. Animals were distributed by age, sex, and weight. Females and males were used interchangeably, but within the *in vivo* infection experimental groups, individuals of the same sex were consistently grouped for comparison. All mice are of the C57BL/6 strain and were bred and housed in a climate-controlled environment at the CNB and CIB in accordance with the sanitary recommendations of the Federation of European Laboratory Animal Science Associations (FELASA). All experimental procedures were approved by the Animal Care and Ethics Committee of the CNB, CIB, and the Complutense University of Madrid (UCM) and by the regional authorities (project nº PROEX 146/18 and PROEX 143.6/20).

BM chimeras

BM WT Cre or HIF-1α KO Cre chimeras were generated by transplanting with 5 × 10^6 BM cells from the WT Ub-Cre ERT2 CD45.2 or the HIF-1$\alpha^{fl/fl}$ Ub-Cre ERT2 CD45.2 mice, respectively, into lethally γ-irradiated (2 doses of 6 Gy) WT C57/BL6 CD45.1 mice. Mixed BM chimeras were generated by injecting a mixture of 5×10^6 BM cells from the RAG1KO and WT Ub-Cre ERT2 or the RAG1KO and HIF-1$\alpha^{fl/fl}$ Ub-Cre ERT2 mice in a proportion of 1:1 respectively, into lethally irradiated WT C57/BL6 CD45.1 mice. After 4 weeks, the reconstituted mice were subsequently treated with tamoxifen. BM WT Cre and HIF-1$\alpha^{fl/fl}$ KO mice mRNA was isolated from peripheral blood to verify the expression of HIF-1α by qPCR. Furthermore, CD4$^+$ T cells from the spleen of the mixed BM chimeras WT Ub-Cre:RAG1KO and HIF-1$\alpha^{fl/fl}$ KO: RAG1KO mice isolated by mouse CD4$^+$ T cell isolation kit were processed to check the expression of HIF-1α by qPCR. Mixed BM chimeras were generated by injecting a mixture of 10×10^6 BM cells from the CD45.2 HIF-1$\alpha^{\triangle Rorc}$ and CD45.1 control mice in a proportion of 1:1, into lethally irradiated WT C57/BL6 mice. After 5–6 weeks, the proportion of CD45.1$^+$ and CD45.2$^+$ was analyzed in blood to decide whether to proceed to infect with *C. rodentium*.

Citrobacter rodentium-induced colitis

To induce colitis with *C. rodentium*, mice aged 8–12 weeks were orally gavaged with 1 × 10^{10} CFU/mL *C. rodentium* strain kindly provided by Dr. Eric Vivier. Survival, body weight, CFUs counts, and tissue histology were assessed as previously described.[56,57] Analysis of CFUs was determined via serial dilutions on MacConkey agar plates supplemented with 0.68% sodium thiosulfate and 0.08% ammonium citrate from mechanically homogenized fecal pellets on days 2, 5 and 12 after *C. rodentium* infection.[58] We performed colon explants and collected a piece of the distal colon to quantify cytokines by ELISA and qRT-PCR respectively on day 12 of the infection. LPCs were isolated for cell sorting, flow cytometry analysis or for being cultured 4 h with brefeldin A to analyze intracellular cytokines.

METHOD DETAILS

Counting of colonic patches

Colons from infected or uninfected mice were collected, washed, and opened longitudinally. Afterward, they were incubated by shaking in phosphate buffered saline solution (PBS) containing 10% Fetal Bovine Serum (FBS), 5 mM EDTA, and 14 mM HEPES at 37°C for 30 min. After washing with PBS, CLPs were counted by backlighting.

Isolation of colonic LPCs

The intestinal lamina propria cells were isolated as described by.[59] In short, mouse colons were removed and cut longitudinally and transversally into 1.5 cm pieces, which were incubated by shaking in PBS containing 10% FBS, 5 mM EDTA, and 14 mM HEPES at 37°C for 30 min. Then, the tissues were then digested in RPMI 1640 containing 10% FBS, 25 mM HEPES, and 300 UI/mL of collagenase

type VII at 37°C for 45 min. The digested tissues were homogenized by passing through 70 μm cell strainers. Mononuclear cells were then harvested from the interphase of a 70% and 40% Percoll gradient after spinning at 2,100 rpm for 20 min at room temperature.

Flow cytometry, antibodies, and ELISA

ILC staining was performed as previously described by.[59] Antibodies against CD45.2, CD3, CD19, Gr-1, F4/80, CD90.2, GATA-3, CD16/CD32, CD127, NKp46, KLRG1, CD4, RORγt, Eomes, IL-17, IL-22, IL-7R, CXCR6, CD5, TCRβ, TCRγδ, CCR6, RORγt and IL-17 were used. For cytokine production, cells were stimulated *ex vivo* by IL-23 (40 ng/mL), IL-1β (100 ng/mL), and Brefeldin A (5 μg/mL) or Stop Golgi (1:1500) for 4 h. For intracellular staining, cells were fixed and permeabilized with eBioscience Foxp3/Factor Staining Buffer Set following the manufacturer's guidelines. For induction of IL-22 through IL-18 stimulation, LPCs were cultivated overnight with or without IL-23 (40 ng/mL) and/or IL-18 (100 ng/mL) followed by 4 h of *ex vivo* Stop Golgi stimulation (1:1500). Flow cytometry analysis and cell sorting were performed on FACSCAria (BD Biosciences), Cytoflex (Beckham Coulter) and Cytek Aurora instruments and analyzed with FlowJo, CytExpert or OMIQ softwares. IL-22, IL-17, and IL-18 in supernatants collected at 0, 3, 5, 7, and/or 12 days after infection were measured by ELISA according to manufacturer's recommendations.

Flow cytometry gating strategy

Th22/Th17 gating strategy: FSC, SSC; singlets, Live Dead−, $CD45^+$, Linage− (F4/80, CD19, Gr-1), $CD3^+$, $CD4^+$, RORγt+. *ILC1 gating strategy:* FSC, SSC; singlets, Live Dead−, $CD45^+$, Linage−, $CD3^-$, RORγt-, Nkp46+, CD127+, Eomes-. *NK cells gating strategy:* FSC, SSC; singlets, Live Dead−, $CD45^+$, Linage−, $CD3^-$, RORγt-, Nkp46+, CD127-, Eomes+. *ILC2s gating strategy:* FSC, SSC; singlets, Live Dead−, $CD45^+$, Linage−, $CD3^-$, RORγt-, Nkp46-, KLRG1+, GATA-3+. *ILC3s Nkp46+ gating strategy:* FSC, SSC; singlets, Live Dead−, $CD45^+$, Linage−, $CD3^-$, $CD4^-$, RORγt+, $CD90^+$, IL7R+, CXCR6+, Nkp46+. *ILC3s Nkp46-/Lti gating strategy:* FSC, SSC; singlets, Live Dead−, $CD45^+$, Linage−, $CD3^-$, $CD4^-$, RORγt+, $CD90^+$, IL7R+, CXCR6+ Nkp46-. *Lti $CD4^+$ cells gating strategy:* FSC, SSC; singlets, Live Dead−, $CD45^+$, Linage−, $CD3^-$, RORγt+, $CD90^+$, IL7R+, CXCR6+, Nkp46-, $CD4^+$. *Lti cells gating strategy*: FSC, SSC; singlets, Live Dead−, $CD45^+$, Linage−, $CD3^-$, RORγt+, Nkp46-, CCR6+. *Non-ILC3 Innate RORγt cells gating strategy:* FSC, SSC; singlets, Live Dead−, $CD45^+$, Linage−, $CD3^-$, $CD4^-$, RORγt+, $CD90^-$, IL7R-, CXCR6-.

Ex vivo organ culture

Colon tissue was harvested from mice, opened longitudinally, and washed in PBS twice. Two biopsy punches (4 mm, Kai medical) from the distal colon were cultured in 400 μL of complete medium (RPMI supplemented with 100 U/mL penicillin, 100 μg/mL streptomycin and 10% FBS) for 24 or 48 h at 37°C. Colons were stimulated with Pam3CSK4 (0.2 μg/mL) + IL-2 (10 U/mL), LPS (1 μm/ML), IL-1β (10 ng/mL), IL-23 (40 ng/mL), TL1A (200 ng/mL), IL-18 (100 ng/mL) and the BP IL-18 (1 μg/mL).

Isolation of splenic ILC3s

Single-cell suspensions were prepared with spleens from the KO HIF-$1\alpha^{\triangle Rorc}$ $EGFP^{+/-}$ and the WT $EGFP^{+/-}$ control mice. Splenic cells were then stained with CD45.2, CD3, CD19, F4/80, and Gr-1. The ILC3s population was also isolated according to its expression of EGFP. Sorted ILC3s were incubated *in vitro* with or without 40 ng/mL IL-23 and/or 100 ng/mL IL-18.

Histology

Colons were cleaned and cut in their distal part. Tissues were fixed in 4% paraformaldehyde and processed for wax embedding. Cross sections of the colon (5 μm) were cut, mounted on slides and routinely stained with hematoxylin and eosin (H&E). Colitis severity was assessed by researchers blinded to sample identity with criteria adapted from X. Wu et al. 2007.[60] This assessment involved a combined score of immune cell infiltration and epithelial damage (crypt loss, hyperproliferation and ulcers). Each parameter graded 0-3 adding on a total score of 12.

Immunofluorescence

Colonic tissues were cut longitudinally, cleaned in PBS and formed into a 'Swiss roll' and embedded in OCT. Tissues were frozen and stored at −80°C, before being sliced into 5-μm-thick sections with a cryostat and fixed in PFA 4% for 20 min. Afterward, tissue sections were permeabilized with PBS containing 0.05% BSA and 0.2% saponin (PBS-Staining buffer) for 30 min at room temperature. After blocking them with PBS-Staining buffer, mice serum (1/100), and Fc block (1/200) for 30 min at 37°C, they were rinsed in PBS and treated with Blockaid for 1 h at room temperature. Subsequently, slides were incubated with anti-EGFP (1/50), anti-CD3 (1/100), and anti-B220 (1/100) for 1 h at 37°C, diluted in the PBS-Staining buffer. After rinsing with PBS, they were stained with goat anti-mouse 488 (1/500), goat anti-rabbit Cy3, and goat anti-rat Ig Alexa 647 in PBS-Staining buffer for 1h 30 min at room temperature. Finally, tissue sections were stained with DAPI (1/500) in PBS-Staining buffer for 30 min at 37°C, washed in PBS1X and mounted with ProLong mounting medium. Images were acquired on a Confocal multispectral Leica TCS SP8 system microscope and Confocal multispectral system Leica STELLARIS 5.

RNA isolation and qPCR

Colonic RNA was purified with TRIzol and reverse transcribed into cDNA. qPCR was performed with QuantStudio 5 Real-time PCR (Applied Biosystems) with PCR Power SYBR Green or MasterMix qPCR ROX PyroTaq EvaGreen in triplicates. Samples were

normalized to the expression of gene encoding 18S. Primers for *Hif-1a, Il-22, Il-18, Slc2a1, Il-17, Il-1b, Il-23p19, Tnf-a, and 18S* (Table S1) were employed.

RNA from sorted splenic ILC3s, cultured with or without 40 ng/mL IL-23 and/or 100 ng/mL IL-18 for 6 h, or from colonic ILC3s of infected mice, was extracted with a RNeasy Micro Kit and was reversely transcribed to cDNA. The qPCR of the genes *IL-22*, *Il-17, Slc2a1* and *Hif-1a* was performed in ''Parque tecnológico de Madrid'', using SYBR Green Supermix. Samples were normalized to the expression of gene encoding 18S.

QUANTIFICATION AND STATISTICAL ANALYSIS

All statistical analyses were performed with GraphPad Prism software. To determine significant differences ($^*p < 0.05$) parametric data were analyzed by two-way ANOVA and 1-way ANOVA followed by Sidak multiple comparisons test, or paired or unpaired Student t-test. For histoscore, 2-tailed Mann– Whitney U test was used. For survival curves, statistics were calculated with the log rank (Mantel-Cox) test.

Cell Reports, Volume *42*

Supplemental information

IL-18-induced HIF-1α in ILC3s ameliorates the inflammation of *C. rodentium*-induced colitis

Ana Valle-Noguera, Lucía Sancho-Temiño, Raquel Castillo-González, Cristina Villa-Gómez, María José Gomez-Sánchez, Anne Ochoa-Ramos, Patricia Yagüe-Fernández, Blanca Soler Palacios, Virginia Zorita, Berta Raposo-Ponce, José María González-Granado, Julián Aragonés, and Aránzazu Cruz-Adalia

Supplemental Figures

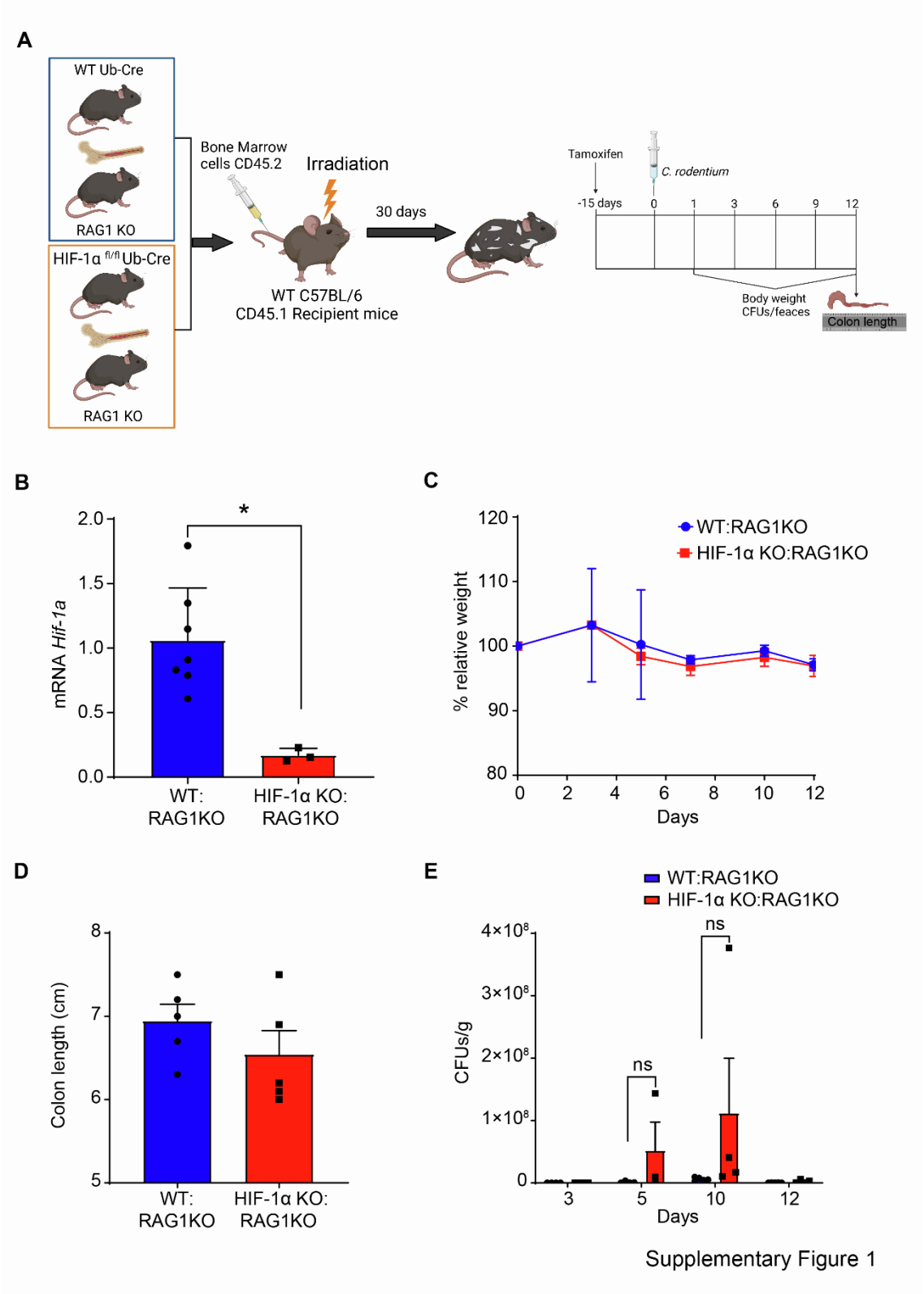

Supplementary Figure 1

Figure S1. Related to Figure 1. HIF-1α in innate cells is essential for protection against *C. rodentium* infection. (A) Schematic image of the generation of the mixed BM chimeras WT: RAG1KO and the HIF-1α KO:RAG1KO mice. (B) Gene expression of *Hif-1a* in isolated splenic $CD4^+$ T cells from the mixed chimeras of RAG1KO and WT (1:1) or RAG1KO and HIF-1α KO (1:1). (C) Relative weight of mixed chimeras of RAG1KO:WT (1:1) and RAG1KO:HIF-1α KO (1:1) following *C. rodentium* infection. (D) Colon length of the mixed BM chimeras after 12 days of the infection. (E) CFUs of *C. rodentium* in the feces of the mixed BM chimeras described in A. The data represent the means ± SD of one representative of 2 independent experiments with n=5. Statistical analysis: (B, D) unpaired-t test; (C, E) two-way ANOVA test. n.s., not significant; *$p < 0.05$. Symbols represent individual animals.

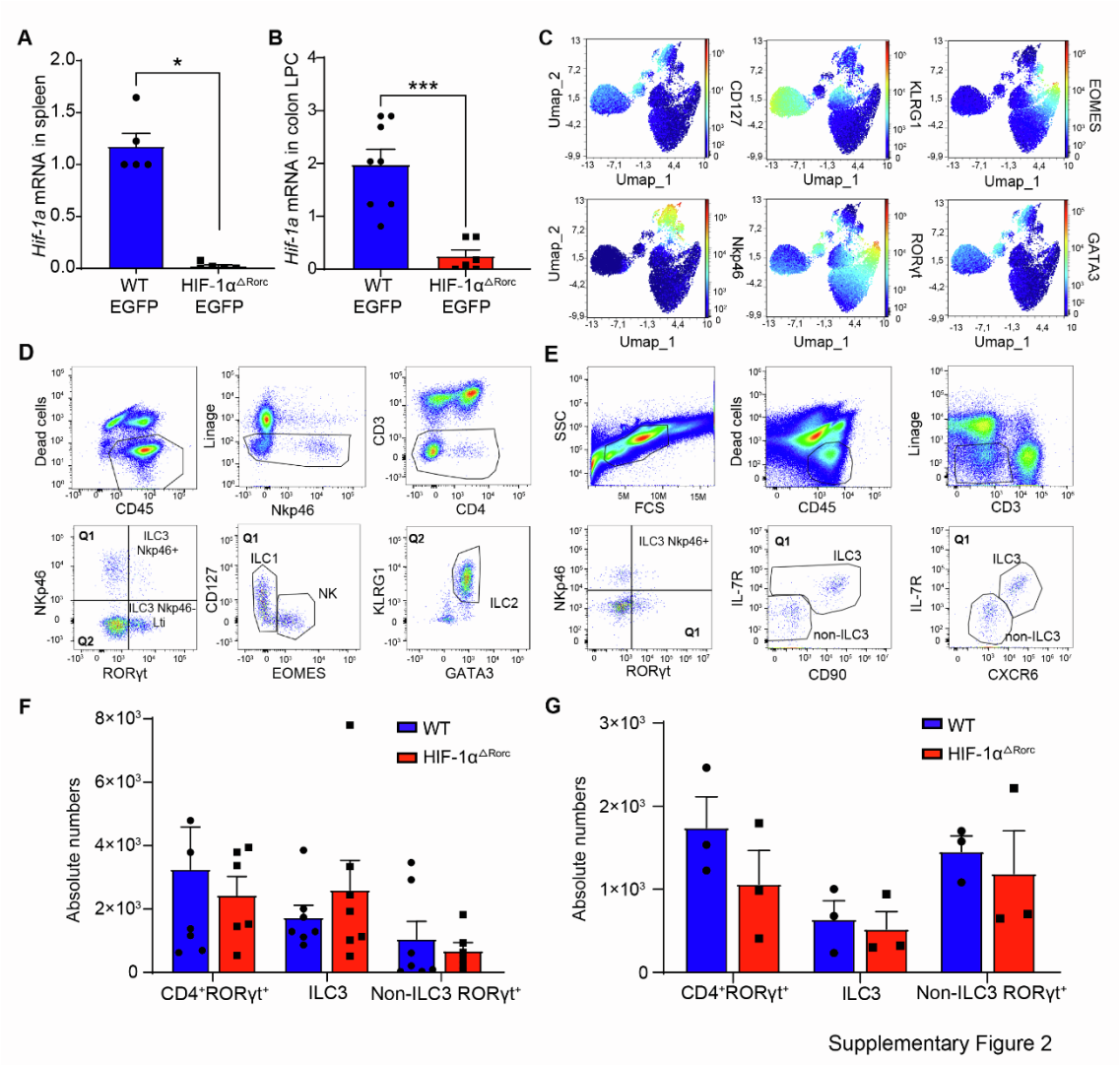

Figure S2. Related to Figure 2. Phenotypic discrimination and analysis of NKs, ILC1, ILC2, ILC3s and other non-ILC3s innate RORγt$^+$ cells in HIF-1α$^{\Delta Rorc}$ and control mice. (A, B) Gene expression of *Hif-1a* in EGFP$^+$ sorted cells from the spleen (A) or colon LPCs (B) of WT EGFP$^{+/-}$ control (blue) and HIF-1α$^{\Delta Rorc}$ EGFP$^{+/-}$ (red) mice. Data represent the means ± SD from (A) four independent experiments and (B) eight independent experiments. (C) UMAP overlays for signature markers. (D) Gating strategy to identify the different ILC subsets in the colon. (E) Gating strategy to identify ILC3s (Lin$^-$, CD3$^-$, RORγt$^+$, CD90$^+$, IL-7R$^+$ and CXCR6$^+$) and the non-ILC3 innate RORγt$^+$ cells (Lin$^-$, CD3$^-$, RORγt$^+$, CD90$^-$, IL-7R$^-$ and CXCR6$^-$). (F, G) Absolute numbers of the different cell RORγt$^+$ populations in the colon (F) or the spleen (G) of the HIF-1α$^{\Delta Rorc}$ and the WT mice in steady state. Data represent the means ± SD from two independent experiments with n= 6 (F) and one experiment with n=3 (G). Statistical analysis: (F, G) Two-way ANOVA with Sidak multiple comparisons. *p < 0.05, ***p < 0.001. Graphs showed individual data.

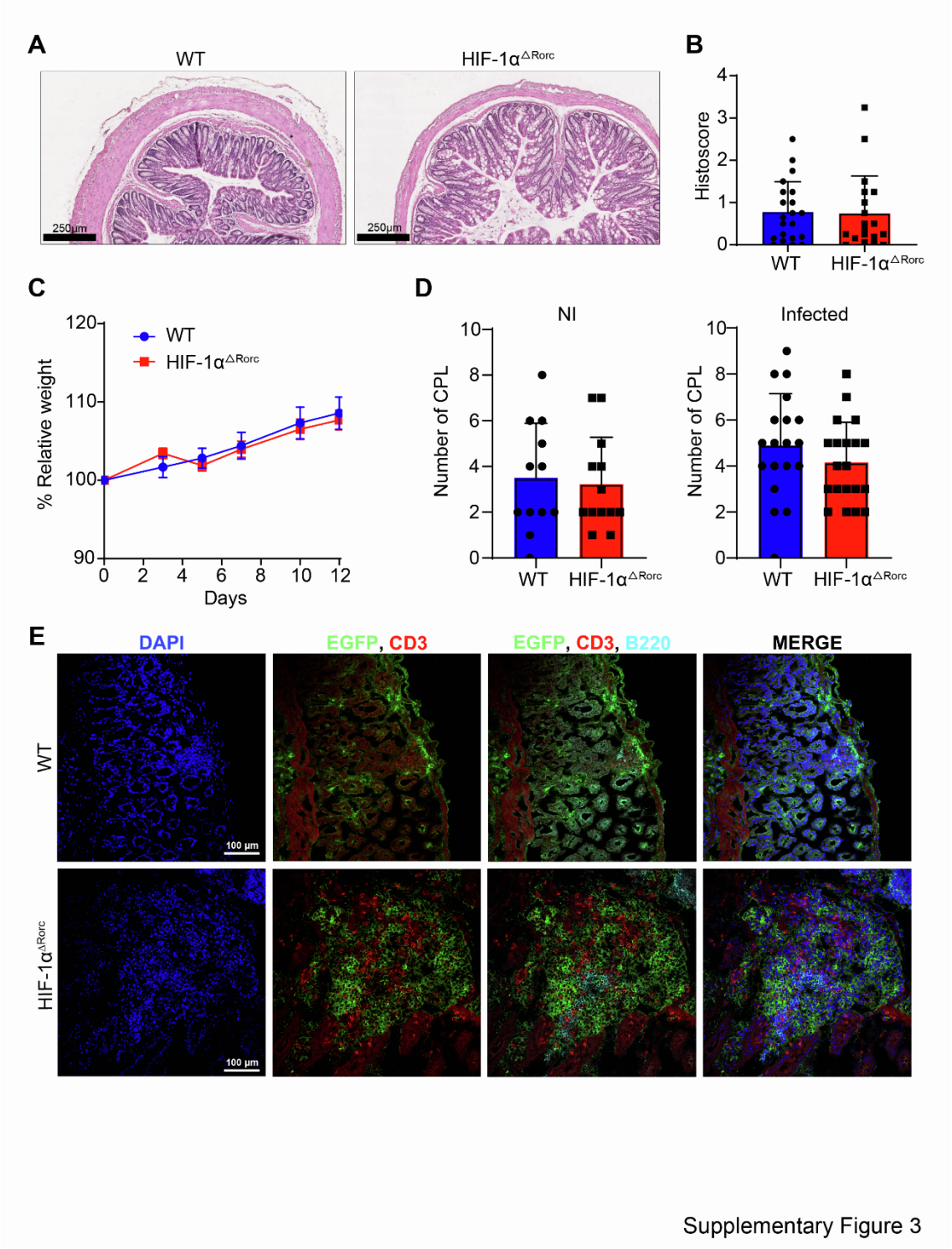

Supplementary Figure 3

Figure S3. Related to Figure 2 and 3. The HIF-1α$^{\Delta Rorc}$ mice do not spontaneously develop colitis in steady state. (A) Representative images of H&E staining on colon tissues from the uninfected WT and HIF-1α$^{\Delta Rorc}$ mice (B) Histoscore of the colitis inflammation in HIF-1α$^{\Delta Rorc}$ and WT mice. (C) Relative weight of HIF-1α$^{\Delta Rorc}$ and WT mice after *C. rodentium* infection. Representative data of three independent experiments. (D) Quantification of colonic patches (CLP) in non-infected (NI) HIF-1α$^{\Delta Rorc}$ and WT mice and after 12 days of infection. (E) Representative confocal images of an immunostaining of colonic lymphoid follicles from the WT

EGFP$^{+/-}$ and the HIF-1α$^{\Delta Rorc}$ EGFP$^{+/-}$ control mice after 12 days of *C. rodentium* infection, showing the RORγt^{+} cells (EGFP), CD3 (red) and B220 (cyan). Data represent the means ± SD of three independent experiments with (B) n= 5 and (D) two experiments of non-infected n=6 mice; three experiments of infected n=6 mice. Statistical analysis: (A) Mann-Whitney U test; (C) Two-way ANOVA, Sidak's multiple comparison test. (D) unpaired-t test. Symbols represent individual animals.

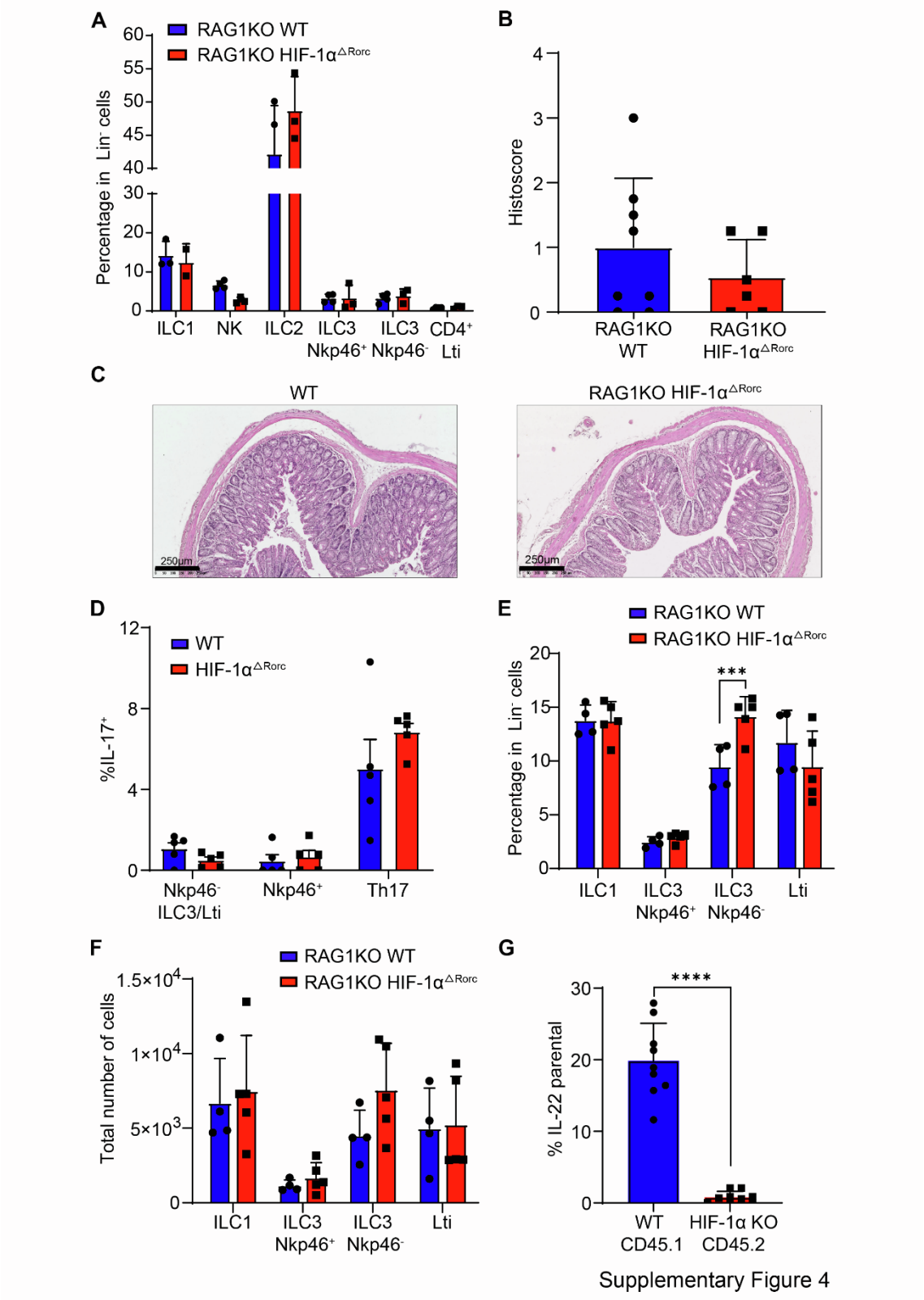

Figure S4. Related to Figure 4 and 5. Colonic ILC populations are unaffected in the RAG1KO HIF-1α$^{\Delta Rorc}$ mice in steady state. (A) Flow cytometry analysis of ILC subsets in the colon from RAG1KO HIF-1α$^{\Delta Rorc}$ and RAG1KO WT control mice. (B) Histoscore of colon inflammation in RAG1KO HIF-1α$^{\Delta Rorc}$ and RAG1KO WT control mice in steady state. (C)

Representative images of H&E staining on colon tissues from the uninfected RAG1KO HIF-1α$^{\Delta Rorc}$ and the RAG1KO WT control mice in steady state. (D) Percentage of IL-17^{+} cells in the different subsets of RORγt^{+} cells detected in isolated colonic LPC cells from the HIF-1α$^{\Delta Rorc}$ and the WT mice after 5 days of *C. rodentium* infection, quantified by flow cytometry. (E, F) Flow cytometry analysis of the percentage (E) or absolute numbers (F) of ILC1 and the different subsets of ILC3s in the colon from RAG1KO HIF-1α$^{\Delta Rorc}$ and RAG1KO WT control mice after 12 days of *C. rodentium* infection. (G) Percentage of IL-22 in the ILC3s from CD45.1 WT or CD45.2 HIF-1α$^{\Delta Rorc}$ detected in isolated colonic LPC cells from chimera mice. The data represent the means ± SD from one experiment with (A) n= 3, (B), from two independent n=4 (D-F) n=5 and (G) n=9 mice . Statistical analysis: (A, E, F) Two-way ANOVA, Sidak's multiple comparison test; (B) Mann-Whitney U test; (D, G) unpaired t test. ***p < 0.001, ****p< 0.0001.

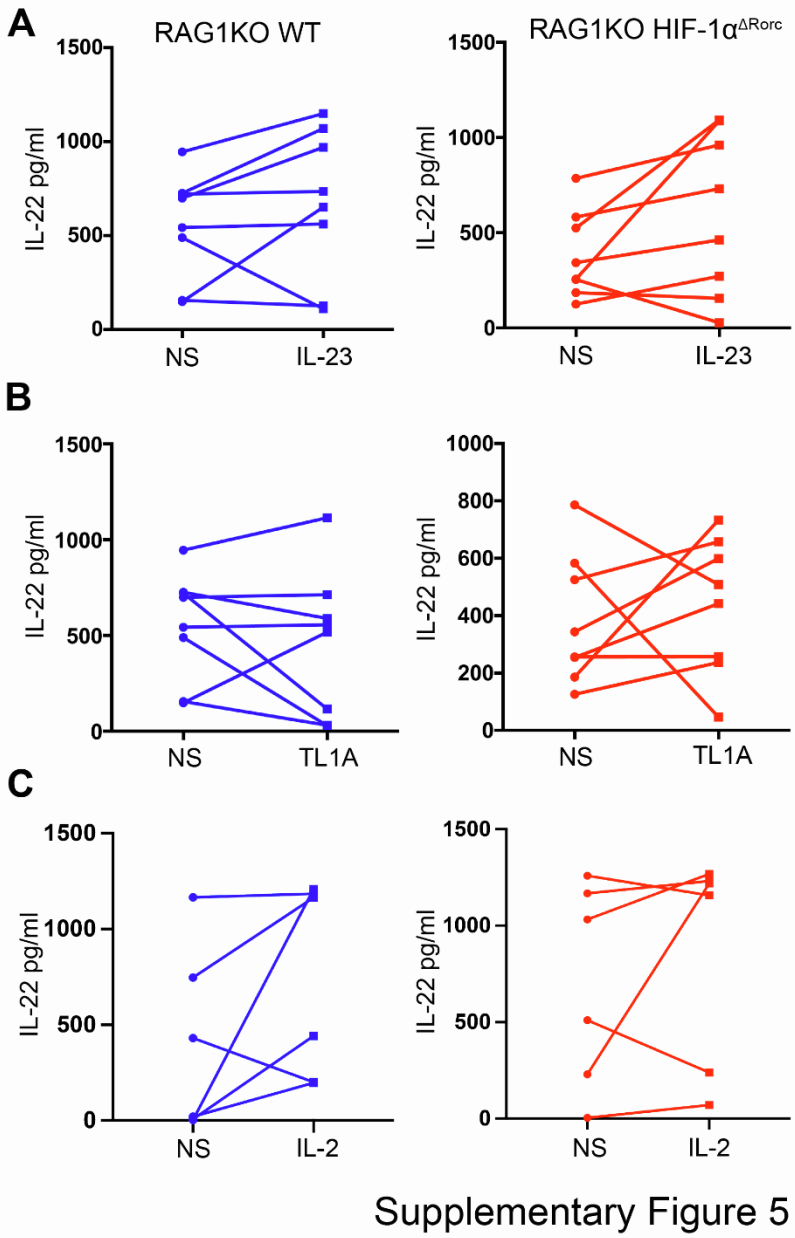

Figure S5. Related to Figure 6. IL-22 secreted by colon explants stimulated with TL1A, IL-23 or IL-2 alone is not significantly higher than non-stimulated colon explants. (A, B, C) IL-22 protein secretion by colon explants from RAG1KO WT (blue) and RAG1KO HIF-1α$^{\Delta Rorc}$ (red) unstimulated (NS) or incubated *ex vivo* with IL-23 (A), TL1A (B) or IL-2 (C) for 48 h. Representative graphics from 3 independent experiments with minimum n=6 mice per group. Statistical analysis: paired-t test.

Table S1. Primer sequences used for qPCR.

Primers qPCR	Sequence
Hif-1a Fw	CACCGATTCGCCATGGA
Hif-a Rv	TCGACGTTCAGAACTCATCTTTTT
Il-1b Fw	AGTTGACGGACCCCAAAAG
Il-1b Rv	AGCTGGATGCTCTCATCAGG
Il-17 Fw	GCAAGAGATCCTGGTCCTGA
Il-17 Rv	AGCATCTTCTCGACCCTGAA
Il-23p19 Fw	ACATCTACCGAAGTCCAATGCA
Il-23p19 Rv	GGAATTGTAATAGCGATCCTGAGC
Tnf-a Fw	ACGGCATGGATCTCAAAGAC
Tnf-a Rv	AGATAGCAAATCGGCTGACG
Il-18 Fw	TACAAGCATCCAGGCACAGC
Il-18 Rv	CTGATGCTGGAGGTTGCAGA
Slc2a1 Fw	CGCCCCCCAGAAGGTTAT
Slc2a1 Rv	TCCGTAGCGGTGGTTCCAT
Il-22 Fw	TCAGCTCAGCTCCTGTCACAT
Il-22 Rv	TCCCCAATCGCCTTGATCTCT
18S Fw	GCAATTATTCCCCATGAACG
18S Rv	GGCCTCACTAAACCATCCAA